Published in final edited form as:
Neuroscience. 2006 December 28; 143(4): 987–1020.

The Thalamic Connections of Motor, Premotor, and Prefrontal Areas of Cortex in a Prosimian Primate (*Otolemur garnetti*)

Pei-chun Fang, **Iwona Stepniewska**, and **Jon H. Kaas***
Department of Psychology ,Vanderbilt University Nashville, TN 37203

Abstract

Connections of motor areas in the frontal cortex of prosimian galagos (*Otolemur garnetti*) were determined by injecting tracers into sites identified by microstimulation in the primary motor area (M1), dorsal premotor area (PMD), ventral premotor area (PMV), supplementary motor area (SMA), frontal eye field (FEF), and granular frontal cortex. Retrogradely labeled neurons for each injection were related to architectonically defined thalamic nuclei. Nissl, acetylcholinesterase, cytochrome oxidase, myelin, parvalbumin, calbindin, and Cat 301 preparations allowed the ventral anterior and ventral lateral thalamic regions, parvocellular and magnocellular subdivisions of ventral anterior nucleus, and anterior and posterior subdivisions of ventral lateral nucleus of monkeys to be identified. The results indicate that each cortical area receives inputs from several thalamic nuclei, but the proportions differ. M1 receives major inputs from the posterior subdivision of ventral lateral nucleus while premotor areas receive major inputs from anterior parts of ventral lateral nucleus (the anterior subdivision of ventral lateral nucleus and the anterior portion of posterior subdivision of ventral lateral nucleus). PMD and SMA have connections with more dorsal parts of the ventral lateral nucleus than PMV. The results suggest that galagos share many subdivisions of the motor thalamus and thalamocortical connection patterns with simian primates, while having less clearly differentiated subdivisions of the motor thalamus.

Keywords

Motor Thalamus; Ventral Lateral Nucleus; Mediodorsal Nucleus; Supplementary Motor Area; Frontal Eye Field

The goal of the present study was to determine the thalamocortical connections of motor and premotor areas of cortex in a prosimian primate known as *Galago garnetti* or, more recently, as *Otolemur garnetti*. Primates represent a particularly interesting branch of mammalian evolution that includes over 200 extant species that are highly varied in body form and behavior (Fleagle, 1999). Most notably, the brain varies in size from about 1.7g in small mouse lemurs to 1250g in the humans (Rowe, 1996). In general, the smaller brains in relation to body size belong to the strepsirhine primates (lemurs, lorises, and galagos) that diverged from the anthropoid primates (monkeys, apes and humans) 60 or more million years ago (Martin, 2004). Given the successful radiation of primates into a number of niches, and the distant separation of the main branches of primate evolution, major differences in brain organization

*Correspondence to: Jon H. Kaas Department of Psychology Vanderbilt University 301 David K. Wilson Hall 111 21st Avenue South Nashville, TN 37203 Tel: (615) 322-6029 (office) (615) 322-7491 (laboratory) Fax: (615) 343-8449 E-mail: Jon.Kaas@vanderbilt.edu

Supported by: NIH grant NS 16446

across taxa can be expected. This is especially the case between prosimian primates such as galagos, with proportionately small brains and more limited behavioral repertoires, and the larger anthropoid primates, such as humans with large brains and impressive behavioral capabilities. Yet, there are certain features that characterize all primate brains, such as having visual areas V1, V2, and MT (e.g., Collins et al., 2001; Lyon and Kaas, 2002), and distinct parvocellular and magnocellular layers in the lateral geniculate nucleus of the visual thalamus (Kaas et al., 1978). Somewhat surprisingly, given the apparent differences in motor performance, galagos (and by implication, other prosimian primates) share a number of subdivisions of motor areas with anthropoid primates, including a primary motor area (M1), a supplementary motor area (SMA), a dorsal premotor area (PMD), a ventral premotor area (PMV), and a frontal eye field (FEF) (Wu et al., 2000). In addition, many of the cortical connections of these areas resemble those of Old World macaque monkeys, where they have been most extensively studied (see Fang et al., 2005 for review). As part of a more extensive effort to see how brains are similar and different across primate taxa, we sought to determine the thalamic connections of motor areas of cortex in galagos in order to compare these connections with those in monkeys. To do this, we determined the distributions of labeled neurons in the thalamus of the same galagos where injections in cortex revealed cortical patterns of connections of motor areas (Fang et al., 2005). As little was known about how the motor thalamus of galagos or other prosimian primates is subdivided into nuclei, it was also necessary to study the architecture of the thalamus in galagos and develop criteria for identifying nuclei in the experimental cases. Thus, the present report includes a description of the architectonic subdivisions of the motor thalamus in galagos, and a description of how these subdivisions project to motor fields of frontal cortex. As injections of tracers into motor fields labeled neurons in the medial dorsal nucleus and intralaminar nuclei, and these nuclei have been associated with the motor thalamus, these nuclei and their connections with motor cortex are described as well.

EXPERIMENTAL PROCEDURES

The thalamic connections of motor, premotor, and prefrontal areas of cortex in prosimian galagos (*Galago garnetti* now known as *Otolemur garnetti*) were determined by placing injections of one or more tracers into one or more cortical areas of eight adult galagos. In these galagos, suitable injection sites in cortex were first identified with microstimulation procedures. After favorable transport times for the tracers, a more extensive microstimulation mapping session was used in each case to further identify motor and premotor areas of cortex, and to define functional boundaries between fields. After euthanasia, the brains were processed so that cortical areas and thalamic nuclei could be identified histologically. The details of the cortical mapping, the placement of injection sites, and cortical architecture are presented in our companion paper on cortical connections in these eight galagos (Fang et al., 2005). Here, we describe patterns of thalamic connections revealed by the cortical injections. Labeled neurons were located in the thalamus relative to nuclear boundaries that were histologically identified in the experimental cases. The galagos came from our breeding colony. All experimental procedures followed the guidelines of the National Institute of Health Guide for the Care and Use of Laboratory Animals, and the guidelines of the Vanderbilt University Animal Care and Use Committee.

Microstimulation and Tracer Injections

Neuroanatomical tracers were injected into various locations in frontal cortex of galagos after appropriate sites were identified with microstimulation. The microstimulation and injections occurred under aseptic surgical conditions while the animals were anesthetized. In preparation for these procedures, galagos were premedicated with robinol (0.015mg/kg, i.m.) and dexamethasone (1-2 mg/kg, i.m.). Animals were then anesthetized with 2% isoflurane. For the

microstimulation session, the frontal cortex of one hemisphere was partially exposed, and the anesthetic was changed to ketamine hydrochloride (30-60 mg/kg/hr, i.v. or 10-30 mg/kg, i.m.) potentiated by xylazine (0.4 mg/kg, i.m.), as the isoflurane suppressed the evoked motor responses. A low impedance (1.0MΩ) tungsten microelectrode was placed in cortical regions of interest and lowered to a depth of 1.5-1.8 mm, approximately the level of layer 5 pyramidal neurons. Monophasic pulses of electrical current in 60 msec trains of 0.2 msec duration per pulse were delivered at 300 Hz to evoke movements. Subdivisions of premotor cortex and motor cortex were identified by the types of movements evoked and the current thresholds needed to evoke movements, as previously described (Wu et al., 2000; Fang et al., 2005).

After injection sites were chosen, different tracers were loaded into the glass micropipettes attached to 1 μl or 2 μl Hamilton syringes. The micropipette was lowered into the identified cortical site, and a tracer was injected at depths of 1.0 mm and 1.5 mm to include both superficial and deep layers. Each galago received up to 4 different tracer injections into different sites (see Table 1). The injections included fluorescent tracers (3% fast blue, FB, Sigma, Inc.; 2% diamidino yellow, DY, Sigma, Inc; 10% fluororuby, FR, Molecular Probes, Inc; or 10% fluoroemerald, FE, in distilled water, Molecular Probes, Inc.). Other tracers were 2% wheat-germ agglutinin conjugated to horseradish-peroxidase (WGA-HRP) (Sigma, Inc.) and 1% cholera toxin subunit B (CTB) (Sigma, Inc.) in distilled water, or 10% biotinylated dextran amine (BDA) (Sigma, Inc.) in 10mM phosphate buffer. According to the sensitivity of the tracers, volumes of 0.03-1.6 μl were injected (see Fang et al., 2005 for details). After injections, the cortex was covered with gelfilm, the opening in the skull was closed with dental acrylic, and the skin was sutured. Precautionary antibiotics were given, and the animals were carefully monitored during recovery from anesthesia.

Four to seven days later, each galago was anesthetized as before, and motor areas of cortex were more extensively mapped to fully define areas and boundaries. Sites of interest were marked with small microlesions. The galago was then given a lethal injection of sodium pentobarbital (60 mg/kg or more). When are flexive, the galago was perfused through the heart with phosphate buffered saline followed by 2% paraformaldehyde in buffered saline, and then 2% buffered paraformaldehyde with 10% sucrose. The brain was removed and cortex was separated from the thalamus for histological processing.

Histology

In order to further identify the locations of cortical injection sites, cortex was flattened as previously described (e.g., Krubitzer and Kaas, 1990) and cut parallel to the surface at 40-50 μm thickness. Sections were routinely processed for myelin (Gallyas, 1979) and cytochrome oxidase (Wong-Riley, 1979). One case was cut sagittally and sections were processed for Nissl substance, myelin, cytochrome oxidase, or non-phosphorylated neurofilament protein using the SMI-32 antibody in order for us to more fully study the cortical architecture (see Fang et al., 2005 for details).The thalamus was cut separately at 40-50 μm thickness in either the coronal or horizontal planes, and sections were processed to reveal the locations of labeled neurons and thalamic architecture. In addition, brain sections that were cut coronally, sagittally, or horizontally from 12 other galagos from previous studies were evaluated to aid the identification of thalamic nuclei and their boundaries. These sections were processed for Nissl substance (cresyl violet), myelin, cytochrome oxidase (CO), acetylcholinesterase (AChE, Geneser-Jensen and Blackstad, 1971), parvalbumin (Pv, Celio, 1990), calbindin D-28K (Cb, Celio, 1990), and the Cat-301 antigen (Hockfield et al., 1983).

For both cortex and thalamus, sections were also processed to reveal the transported tracers. Sections for fluorescent tracers were mounted unstained (typically every 4th section). Depending on which tracers were injected, similar sets of sections were processed for WGA-HRP (Gibson et al., 1984), BDA (Veenman et al., 1992), or CTB (Bruce and Grofova, 1992).

Data Analysis

Neurons labeled with fluorescent tracers were plotted at high magnification using a fluorescent microscope coupled to an X-Y encoder and a Macintosh G3 computer running Igor Pro software (Wave Metrics, Inc.). Neurons labeled with WGA-HRP, BDA or CTB were similarly plotted using dark- or bright-field illumination. Blood vessels and other landmarks were identified on the plots so that plots of labeled neurons could be aligned locally and accurately with drawings of adjacent sections processed to reveal architectonic borders. Thalamic sections from the present experimental cases, and those from other studies that were processed for AChE, myelin, CO, Pv, Cb, or Cat-301 antigen were examined on a bright-field microscope or projector. After a detailed review of architectonic distinctions across preparations, thalamic nuclei were identified in brain sections from the experimental cases and boundaries of nuclei were transfered onto sections with plots of labeled neurons.

Images of plotted sections were processed using Canvas 7.0 software (Deneba, Inc.). Digital photographs of brain sections were captured using a Spot 2 digital camera (Diagnostic Instruments, Inc.) mounted on a microscope. The digital images were adjusted for brightness and contrast using Canvas software, but they were not otherwise altered.

RESULTS

The results are presented in two parts. In the first part, we describe the architecture of the motor and adjoining thalamus of galagos. This is a critical component of the present study as divisions of the motor thalamus have not been described in detail in prosimian primates (but see Simmons, 1980; Jones 1985, 1998a, 1998b), and any description of thalamocortical connections depends on identifying the relevant subdivisions of the thalamus. In contrast, subdivisions of the motor, premotor, and prefrontal cortex have been well-described in previous studies in galagos (e.g., Preuss and Goldman-Rakic, 1991; Wu et al., 2000; Fang et al., 2005), and a detailed description of cortical areas is not needed here. Part two of the results focuses on the distributions of labeled cells in the thalamus after injections of tracers into M1, PMV, PMD, SMA, FEF, and prefrontal cortex. The subdivisions of motor cortex were defined in the present cases as reported in our previous study of cortical connections (Fang et al., 2005).

Architectonic subdivisions of the motor thalamus in galagos

In New and Old World monkeys, several basic subdivisions of the motor thalamus are generally distinguished (see Stepniewska et al., 1994a). These include ventral anterior (VA), ventral lateral (VL) and ventral medial (VM) nuclei. In VL, anterior (VLa) and posterior subdivisions have been distinguished, and the posterior subdivision is further divided into a principal nucleus (VLp), a medial nucleus (VLx), and a dorsal nucleus (VLd). Other terms have been applied, but the subdivisions for New World owl monkeys (Stepniewska et al., 1994a) correspond closely with those in current use for macaque monkeys (Table 3), although VLd, VLx and VLp are sometimes included within an undivided posterior VL (e.g. Jones, 2001). While coronal brain sections are most commonly used to illustrate subdivisions of the thalamus, the main components of the motor thalamus are distributed rostrocaudally, so their distinction is more evident in sections cut in the sagittal or horizontal planes. Our analysis of thalamic architecture in sections cut in different planes in galagos has shown that subdivisions of the motor thalamus are best distinguished in sections cut in the horizontal plane. Thus, the architecture of the motor thalamus is illustrated mainly in photomicrographs of horizontal sections. The plane of section is especially important in galagos, since the subdivisions of the motor thalamus are less distinctly differentiated than in monkeys. Although sections processed for a number of different markers were examined in this study, sections processed for AChE were especially useful in

revealing the relevant thalamic subdivisions. In addition, sections processed for cytochrome oxidase (CO) or parvalbumin (Pv) were also helpful.

The location of the motor thalamus is apparent in low magnification photomicrographs of horizontal brain sections stained for AChE (Fig. 1). Dorsally (Fig. 1A), only a small part of the motor thalamus (MoT) is apparent. This part of the motor thalamus is wedged between the more lateral reticular nucleus (Rt), the more medial, relatively large anterior thalamus (ANT), the intralaminar nuclei (IL), and the posteriorly located lateral posterior nucleus (LP). The large pulvinar complex (Pul) occupies the posterior thalamus, just anterior to the superior colliculus (SC). The mediodorsal nucleus (MD) is a conspicuous medial structure. More ventrally (Fig. 1B), sensory nuclei dominate the thalamus. The motor thalamus extends just anterior to the darkly-stained ventroposterior (VP) somatosensory nucleus, which is subdivided by lightly-stained septa. The lateral geniculate nucleus (LGN) and the medial geniculate nucleus (MGN) are posterior to VP.

Subdivisions of the motor thalamus are apparent in horizontal brain sections examined at a higher magnification, especially in sections processed for AChE (Fig. 2). In this preparation, the motor thalamus can be divided into three main regions. A ventral anterior region (VA) is located just posterior to the anterior nuclear complex (ANT), and medial to the reticular nucleus (Rt). The VA region can be divided further into a lateral parvocellular portion or nucleus, VApc, and a medial magnocellular portion, VAmc. The adjoining ventral lateral region includes anterior (VLa) and posterior (VLp) nuclei. The ventral medial (VM) region or nucleus is not distinct, and it is not clearly subdivided. The histological features of these nuclei are described below.

Ventral lateral region, posterior nucleus (VLp)

The territory of the VLp is larger than that of adjacent VLa. In all planes, VLp has a distinctive appearance that allows it to be distinguished from neighboring nuclei. In AChE, CO, and Pv preparations, VLp can be identified as a darkly stained structure. In Nissl and myelin preparations, VLp can be divided further into medial and lateral subdivisions, based on slightly different architectonic characteristics.

Processing for AChE reveals the most distinctive histological feature of VLp, a dense and dark reticular pattern that probably reflects the presence of AChE enzyme in the endothelial cells of the capillary walls (Fig. 2, 3A). Moreover, the neuropil is unevenly stained as a result of lightly stained bundles of fibers that course mediolaterally through the nucleus (Fig. 2 and 5C). A few AChE-stained cell bodies are distributed among the darkly stained capillaries in VLp (Fig. 3A). The neuropil and capillaries are a little darker in the medial part of the VLp than in remaining VLp. In Nissl sections, VLp is characterized by cells of different sizes and shapes, that are unevenly distributed throughout this region (Figs. 5A, 6A, and 7A, see also Fig. 11C and D). In the medial sector of VLp adjacent to the intralaminar nuclei (Fig. 4D), the cells are slightly larger than those in the central sector. The central VLp contains medium-sized cells that are slightly larger than those in the lateral sector adjacent to the reticular nucleus (Rt). The cells in the medial and central portions of VLp are round while the lateral VLp contains smaller-sized cells that are elongated in shape. These cells in the lateral VLp are clustered into groups distributed among thick fiber bundles (Fig. 5C). Thus, from medial to lateral VLp, cells become smaller and less uniformly distributed. In addition, the cells in the dorsal VLp are larger and more densely packed than those in the ventral VLp, which contains smaller, irregular-shaped and loosely-packed cells. Thus, there are suggestions of the lateral, medial and dorsal subdivisions within VLp.

In Nissl preparations, the cells in VLp are larger, sparser and less uniformly distributed than cells in the more posterior and dorsal LP nucleus, so it is not difficult to distinguish VLp from

LP (Fig. 7A). More ventrally in the thalamus, loosely packed VLp cells contrast with the densely packed cells in VP, so VLp and VP are easily distinguished. Between lateral VLp and VP, there is a region sparsely populated with neurons that does not appear to correspond with either nucleus. The cells in VLp are slightly bigger and more darkly stained than the cells in VLa, which is located anterior to VLp (Fig. 4C,D).

In myelin stained sections (Fig. 5C), fibers in VLp are densely packed with the fiber bundles in the lateral part that are thicker and sparser than the fibers in the medial part. The myelin pattern in VLp is similar to that in VLa, but the fiber bundles in VLa are thicker and somewhat denser than in VLp (Fig.5C). The border of VLp with VP is clearly marked because the ventral VLp contains denser and darker fibers and VP contains more lightly stained thinner fibers. Poorly myelinated septal regions divide VP nucleus into subnuclei.

In sections processed for Pv or CO, VLp contains a dark to moderately dark neuropil with some darkly stained cell bodies (Figs. 5B, D, 6C and 7B). VLp appears as a structure that is easily distinguished from the rostrally adjacent lighter structures such as VLa and VA. Dorsally, the posteriorly adjacent LP is pale in CO and Pv preparations, in contrast to darkly stained VLp (Fig. 7B). However, at the ventral levels, VP is just slightly darker than VLp.

Ventral lateral region, anterior nucleus (VLa)

The anterior subdivision of the VL complex, VLa, is smaller than VLp, and it protrudes into the ventral anterior region (VA) that surrounds VLa anteriorly (Fig. 2). Laterally, VLa is adjacent to the reticular nucleus (Rt), anterior to VLp nucleus, and dorsal to VM. VLa is seen most clearly in the AChE preparations, whereas VLa is not that apparent in other preparations such as CO and Pv.

In AChE preparations, VLa is distinguished by moderately to darkly stained cell bodies and lightly stained neuropil (Fig. 2, 3B). Lateral VLa has a somewhat darker neuropil that resembles the neuropil in the lateral subdivision of VA. Thus, in less than favorable sections, it is difficult to distinguish lateral VLa and VA. VLa lacks the reticular pattern formed by the stained capillaries in VLp, so distinguishing between the two nuclei is not difficult. In Nissl preparations, VLa contains mostly small cells (Fig. 4C). Most of these cells are oval in shape, but some are round and multipolar. The cells in VLa are not uniformly distributed, but form loosely arranged clusters. In favorable sections, it is quite easy to delineate the posterior border of VLa, since the cells in posteriorly adjacent VLp are larger and more darkly stained (Figs. 4C,D, 5A and 6A). The anterior border with VA is more difficult to establish, especially with lateral VApc, since the cells in both nuclei are similar in size (Fig. 4A, C). In general, the cells in the VLa are smaller than in the ventral anterior region, especially its medial magnocellular part (VAmc) (Fig.4B,C). The VLa-VAmc border is marked by larger and more uniformly-arranged neurons in VAmc (Fig.4 B, C). In myelin stained sections, densely packed bundles of darkly stained fibers are found in VLa (Fig.5C). While a border between VLa and VLp is not always clear; the border between VLa and VA is apparent as fiber bundles in VLa are somewhat thinner and denser than in VA. Pv and CO preparations display VLa as a lightly stained structure (Figs. 5B, D and 6C). In both preparations, the neuropil in VLa is as light as in VA and much lighter than the dark posteriorly adjacent VLp. Thus, the VLa border is more apparent with VLp than with VA. Another feature that distinguishes VLa from VLp in Pv and CO preparations is the presence of large, darkly stained cell bodies in VLp.

Ventral anterior region (VA)

The ventral anterior region (VA) is located in the most anterior part of the motor thalamus that is surrounded by the reticular nucleus (Rt). VA is much smaller than the VL region. In AChE preparations, moderately-to-darkly stained patches of neuropil distinguish the VA region from

neighboring nuclei, and VA is darker than VLa, but lighter than VLp. Medial VA (VAmc) has somewhat lighter neuropil than lateral VA (VApc). Sections cut in the horizontal and sagittal planes (Figs. 2, 6) were most useful in distinguishing VA from VL. In the coronal sections, VA is difficult to delineate from neighboring structures.

In Nissl preparations, cells in lateral VA (VApc) are smaller and more elongated than those in medial VA (VAmc) (Fig. 4A, B and 5A). VAmc contains round cells that are also larger than the cells in the VL region. In myelin preparations, VA is sparsely packed with thick fiber bundles that are more lightly stained and more sparsely distributed in medial than in lateral VApc (Fig.5C) In Cb preparations, the VA region is quite homogeneous and moderately stained. However, in CO and Pv preparations, VA is a heterogeneous structure. In CO preparations, VApc is more darkly stained than VAmc and the posteriorly adjacent VLa (Fig. 5B), especially at the dorsal levels. At the ventral levels, both VAmc and VApc are moderately and homogeneously stained. In PV preparations, VA has a patchy pattern with VAmc being darker than VApc (Fig. 5D). As VApc resembles VLa, the border between VLa and VApc is not clearly marked.

Ventral medial nucleus (VM)

The ventral medial nucleus (VM) is located ventral and medial to VL region. VM is most clearly demarcated from the neighboring structures in AChE and Pv preparations where VM is a homogeneous structure that is lighter (Fig. 6C and 7B) than adjacent structures, such as VLp or VLa. The cell bodies in VM are less darkly stained than in either VLp or VLa (Fig. 7A). The borders of VM are best appreciated in sections cut in coronal plane. In the sagittal plane, the border between VM and VLa is difficult to distinguish.

In Nissl preparations, VM has mostly multipolar but also round cells that are evenly distributed and less darkly stained than those in VLa and VLp (Fig. 6A). In myelin stains, VM is characterized by thin fibers that are lightly stained and densely packed. The myelin pattern in VM is not very different from that in VL, so the VM-VL border cannot be marked with certainty. In both CO and Pv preparations, VM is lightly to moderately stained and similar in appearance to VA and VLa, but different than the darkly stained VLp (Fig. 6C).

Other motor-related thalamic nuclei

Although ventral lateral, ventral anterior, and ventral medial thalamic regions are the main source of projections to the motor cortical areas, other nuclei in the thalamus that are related to motor movements also send inputs to areas of motor cortex. In the present study, labeled cells were seen in the intralaminar nuclei (IL) and medial dorsal nucleus (MD) after neuroanatomical tracers were injected into the primary motor area and premotor areas.

The intralaminar nuclei (IL)—Intralaminar nuclei are embedded within internal medullary lamina and involve paracentral (Pc), central lateral (CL), centromedian (CM), and parafascicular (Pf) nuclei. Pc and CL are located in dorsoanterior thalamus, whereas CM and Pf are located ventroposteriorly. Both Pc and Pf are fairly small structures compared to CL and CM. In order to differentiate the IL nuclei, it is useful to consider more than one plane of section and more than one staining method. Pc is better viewed in the horizontal and sagittal planes, whereas horizontal and coronal planes better reveal CL.

In AChE preparations, Pc has a darkly stained neuropil with a few stained capillaries. In contrast, CL is a lightly stained structure with a neuropil that is loosely packed with AChE dark patches and few darkly stained cell bodies at more posterior levels. In Nissl preparations, Pc contains densely packed and moderately dark elongated cells of medium size, while CL contains loosely packed cells that are smaller and lighter stained. There are more multipolar

cells in the dorsal part of CL, and more elongated cells in the ventral part of CL. The elongated cells are loosely packed with the long axis parallel to adjacent structures. CO, Pv, Cb and Cat 301 preparations reveal Pc and CL as medium-dark structures. The myelin pattern of Pc is similar to that of the adjacent motor thalamic nuclei, whereas CL is densely packed with darkly stained, elongated fibers that distinguish CL in horizontal sections from adjacent VLp and MD. In general, the borders between Pc and CL are not very distinct.

The other two IL nuclei, CM and Pf, are located in the posterior thalamus just ventral and posterior to MD. CM is large compared to other IL subdivisions A thin septum that separates CM from adjacent structures is apparent in all planes (Figs. 5, 6, 8A and B). Pf is smaller than CM and is located medial to CM. The horizontal plane shows Pf better than the coronal plane. In AChE preparations, CM has an uniform and quite darkly stained neuropil (Fig. 6B), which makes CM easy to distinguish from VP and MD. AChE preparations best define Pf, as PF is characterized by darkly stained cell bodies and a moderately stained neuropil. In Nissl-stained sections, CM has medium-sized multipolar and irregular-shaped cells. These cells are evenly distributed and darkly stained. The cells are slightly larger than those in CL, but close in size to the cells in VP and MD (Fig. 5A, 6A and 8A). Pf has small elongated and oval-shaped cells. These cells are somewhat darker and more densely packed than cells in CM (Fig. 8A). CO, Pv and Cat 301 preparations reveal CM as a uniformly moderately-stained structure, which contrasts to the darker stained CL and the most lateral part of MD (Fig. 5B, 6C and 8B). Similarly, Pf is a distinctive, dark, oval-shaped structure in CO, Pv and Cat 301 preparations. In myelin-stained sections, CM and Pf have moderately stained fine fibers that mingle and fill both structures.

The medial dorsal nucleus—The medial dorsal nucleus (MD) contains three subdivisions: a medial magnocellular division (MDmc), a central parvocellular division (MDpc), and a lateral multiform division (MDmf). The subdivisions of MD are best seen in the coronal and horizontal sections. MDmc is somewhat smaller than MDpc (Fig. 8). The smallest division of MD, MDmf, is elongated anterioposteriorly along the border with IL.

Subdivisions of MD are clearly revealed in AChE, CO, Pv and Cat 301 preparations (Fig. 8). The central MDpc is the most darkly stained subdivision in AChE (Fig. 8C), and quite pale in Pv (Fig. 8D) preparations. MDpc contrasts with medially adjacent MDmc, which is less dark in AChE, but darker in Pv and CO preparations. The smallest and most lateral MDmf subdivision is distinguished from MDpc by a darker appearance in Pv and CO preparations, and a lighter appearance in AChE preparations (Figs. 7B, and 8C and D). The most caudal part of MDmf has a darker, patchy pattern in Cat-301 preparations (Fig. 8B).

The overall MD region looks pale in Cb preparations. In myelin-stained sections, the borders separating the three MD subdivisions are not clear. However, the fibers in the lateral MD (mostly in MDmf) are thinner, more densely packed, and more lightly stained than the fibers in the medial MD (mostly in MDmc).

In Nissl stained sections, the most lateral MDmf is densely packed with medium-sized cells (Fig. 6; 8A). These cells are mostly oval in shape, multipolar, or round, and are evenly distributed. MDpc contains small-sized cells of irregular shapes. These densely-packed cells are smaller than those in MDmf. MDmc is composed of darkly stained cells. Most of these cells are round and multipolar but some are irregularly shaped. The cells in MDmc are larger and more loosely packed than the cells in MDpc and MDmf.

Thalamocortical connections

Patterns of thalamic connections were revealed by placing injections of tracers in motor and premotor areas and relating the locations of retrogradely labeled neurons to histologically defined thalamic nuclei. Results were obtained from eight galagos with 2-4 injections in M1, PMD, PMV and SMA (Table 1). These cortical areas are located just anterior to somatosensory cortex (Fig. 9A). The locations of injection sites in these areas (Fig. 9B) are shown in more detail, along with the resulting distributions of labeled neurons in cortex, in Fang et al. (2005).

Injection sites typically involved nearly all cortical layers. The injection core of dense uniform label was usually about 1-1.5mm in diameter, surrounded by a ring of labeled neurons or axons and neurons, with some variability depending on the tracer. WGA-HRP injections, for example, produced a dense core surrounded by labeled cells and axons (Fig. 10A). The resulting label in the thalamus included foci of both labeled cells and axon terminals (Fig. 10B), but the labeled neurons could be distinguished from labeled axon terminals when these foci were examined at higher magnification (Fig. 10C). Only the labeled neurons were plotted, although distributions of labeled neurons and labeled terminals were highly congruent. Other tracers also effectively labeled thalamic neurons. The appearance of the labeled neurons varied somewhat with the type of tracer. Figure 11 provides examples of thalamic neurons labeled by FR (A), DY (B), BDA (C) and CTB (D). The distributions of thalamic neurons that were labeled by these injections indicate that each motor area receives inputs from several thalamic nuclei while receiving major inputs from a different region of the VL complex. In general, premotor areas receive inputs mainly from anterior parts of the VL complex (VLa and anterior VLp), and M1 receives inputs from posterior parts of the VL complex (posterior VLp). Moreover, dorsal premotor cortex (PMD) receives major inputs from dorsal VL, and ventral premotor cortex (PMV) from ventral VL. The distributions of labeled cells resulting from individual injections are described below.

Thalamocortical Connections of M1

Eight injections were placed in M1. Based on the results of microstimulation (Fang et al., 2005), five of the injections were placed in the middle sector of M1 that represents the forelimb, two were placed in the lateral representation of face and tongue, and one was in the more medial representation of the trunk and hindlimb (Table 1). The results reveal both, what thalamic structures project to M1, and what portions of these structures project to different parts of M1.

The most medial injection (CTB) involving M1 was in the rostral part of the trunk representation, with some involvement of the forelimb representation and probably the hindlimb representation (Fig. 9B, case 03-65). This injection may have extended slightly into SMA. The injection labeled large numbers of neurons in the motor thalamus (Fig. 12). The labeled cells were widely spread in VLp and VLa nuclei, although they were concentrated in the posterior and lateral parts of these nuclei. Labeled neurons were also found more posteriorly in the lateral posterior nucleus (LP). Only few labeled neurons were found in VA and VM. In addition to the motor nuclei, many labeled neurons were in IL (Pc and CL), and some were in CM, the anterior pulvinar, MDmf, and the midline nuclei (MIN). These results suggest that medial M1 receives dense inputs from VLp, VLa, and IL, and sparser inputs from several other nuclei. The widespread distribution of labeled neurons likely reflects the large size of the injection core and the possible involvement of SMA.

Five galagos received tracer injections into the forelimb representation of M1 (Table 1). Results are shown for three cases. In galago 03-74, an injection of FE was restricted to a small portion of the forelimb representation in M1 (Fig 9). As a result of the more restricted injection, fewer neurons were labeled in the thalamus, compared to the larger injection in galago 03-65 with

an injection in the trunk region. The densest focus of labeled neurons was in the middle of the posterior part of VLp (Fig. 13-1), with a few labeled neurons scattered through its anterior part. The second focus of label was in VLa, mostly its posterior region. Only a few labeled cells were in CM, VP and anterior pulvinar. Similar results were obtained in case 99-75 after an injection of WGA-HRP that covered the caudal portion of M1 (Fig. 9B). In coronal brain sections, a large, dense focus of labeled neurons was in central and ventral VLp (Fig 13-2 left). A second focus was in VLa, mostly the posterior part. In a third illustrated case, galago 00-79 (Fig. 13-2 right), a large injection of DY involved much of the forelimb portion of M1 (Fig. 9B), while extending slightly into PMD and area 3a. In coronal sections, a dense focus of labeled neurons was again located in central and ventral VLp, spreading somewhat posteriorly into the anterior pulvinar. As in two other cases with M1 forelimb injection, a separate quite dense focus of labeled cells was in VLa, and some label was in IL. Few labeled cells were also found in VP and ventral MD. The results from the other two cases (not illustrated) with injections in the forelimb portion of M1 were similar in that the bulk of labeled neurons were in VLp. Other labeled neurons were in VLa, and a few labeled cells were in other nuclei.

Labeled cells were counted and assigned to nuclei in case 03-74 (Fig. 13-1), as the injection was wholly confined to forelimb M1. The thalamus was cut in the favorable horizontal plane, which allowed subdivisions of the motor thalamus to be more clearly distinguished. Of 341 labeled neurons in the motor thalamus, 260 (76%) were in VLp and 81 (24%) were in VLa (Table 2).

Overall, results from five cases indicate that the majority of the projections from the motor thalamus to the forelimb portion of M1 originate from the VLp. Another important, but less dense projection arises from posterior VLa. Of the other motor-related thalamic nuclei, the IL nuclei provide a major contribution to the motor cortex. The labeled neurons in MDmf in case 00-79 may have resulted from a slight involvement of the injection in PMD.

An injection was placed in the orofacial representation of M1 in two galagos. A DY injection in galago 03-65 produced a large injection core (Fig. 9B) that included much of the orofacial region, while extending slightly into the forepaw representation of M1. In addition, the core extended posteriorly into area 3a, and anteriorly into PMV, although these areas were only slightly involved. The neurons labeled by this injection, as viewed in horizontal brain sections (Fig. 14-1), were most dense in a large posterior-medial sector of VLp. A second dense focus was in the medial VLa. IL nuclei, especially posterior CL and CM, were heavily labeled, and adjacent MDmf contained a significant amount of labeled cells as well. Some labeled neurons were also present along the midline (MIN). Other labeled neurons were in the ventroposterior complex, VP, and the anterior pulvinar (PA), possibly reflecting the extension of the injection core into area 3a of somatosensory cortex. The other injection in the orofacial sector of M1 also produced a large central core of presumed tracer uptake, but the distribution of labeled neurons in the thalamus was more restricted. In a series of coronal sections, most of the labeled neurons were in the most ventromedial portion of VLp, with some spread into VM (Fig. 14-2). A second, smaller focus was more anterior in medial VLa. Again some labeled neurons were in the posterior IL and CM. Only an occasional labeled neuron was located elsewhere in the thalamus. The results from these two cases, but especially those from case 99-75, suggest that the main thalamic contribution to the orofacial sector of M1 comes from VLp, with a smaller contribution from VLa. As mentioned above, the labeling of neurons in the somatosensory nuclei of VP and anterior pulvinar of case 03-65 may reflect the involvement of somatosensory cortex (area 3a) in the injection site, while the spread of the injection core into the forepaw portion of M1 may account for the more widespread distribution of labeled neurons in VLp and VLa.

Across all eight cases with M1 injections, the results indicate that VLp provides the major inputs to M1 from the motor thalamus. VLa provides a secondary source of inputs from the motor thalamus. Within VLp, the trunk representation in M1 receives more inputs from the lateral portion of this nucleus, the forelimb representation from the medial part, and the orofacial representation from the most medial part. The projections from VLp to the orofacial portion of M1 are also from the most ventral part of VLp. Of the other thalamic nuclei, IL nuclei have quite dense projections to M1.

Thalamic Projections to PMD

Tracers were injected into nine locations in PMD in seven galagos. Six of the injections were placed in PMDc (caudal PMD) and the injection cores in all six appeared to be confined to PMD. Three injections were in PMDr (rostral PMD), with one core extending slightly into adjoining prefrontal cortex and possibly FEF.

In galago 03-65, an injection of CTB was restricted to the anterior portion of PMDc that is devoted to forelimb movements (Fig. 9B). In horizontal sections, labeled neurons were concentrated in medial VLa and VLp, especially in the dorsal portions of these nuclei (Fig. 15-1). At least in some brain sections, the labeled cells in these two nuclei appeared to form separate foci. In VLp, the labeled neurons were mostly concentrated in the anterior portion, according to the level of the horizontal sections. The numbers of neurons labeled in VLa (355, 46%) and VLp (348, 46%) were very similar (Table 2). Other labeled neurons were in lateral VA (VApc), and very few were in the ventro-medial part of the motor thalamus, probably involving VM. IL contained a significant amount of labeled cells in a more rostral part of IL than that labeled by M1 injections. Some neurons were clustered in MDmf, along the midline (MIN), and a few labeled neurons were also in the lateral posterior nucleus (LP) and the anterior pulvinar. The results suggest that VLa and VLp project to PMDc in nearly equal densities, while IL provides a third substantial input.

In galago 03-74, an injection of CTB that was confined to the medial forelimb in PMDc (Fig. 9B) produced a somewhat denser and wider distribution of labeled neurons in the thalamus (Fig. 15-2). In the motor thalamus, VLp contained the most labeled neurons (51%) and VLa had the next densest projection (38%). The labeled cells were widely distributed in the dorsal parts of these nuclei, and they were concentrated in the medial parts. Some cells were labeled in the lateral VA (VApc) and in VM. Many labeled neurons were in IL, CM, MDmf, midline nuclei (MIN), and some neurons were in the LP-Pulvinar region. The somewhat wider distribution of labeled neurons in this case than in other cases with PMDc injections raises the possibility of a slight involvement of SMA and/or PMDr in this medial PMD injection.

After an injection of FR in caudomedial PMDc in galago 99-75 (Fig. 9B), cells were labeled in VLa and VA (VApc), and in the middle and medial portion of rostral VLp (Fig. 15-3). Sparser label was seen in VM. Outside the motor thalamus, labeled neurons were scattered in posterior CL, and few were in CM. Caudal and lateral MD (MDmf) contained a number of labeled neurons. Galago 00-79 and 01-123, with an injections of WGA-HRP centered in PMDc, were also cut in the coronal plane (not shown). Fewer neurons were labeled by these injection than by other injections in PMDc, but dense foci of labeled neurons were located in VLa and VLp, with slightly more in VLa. As in other cases with PMDc injections, labeled neurons were found in IL and lateral MD (MDmf) (not shown).

In summary, the major projections from the motor thalamus to PMDc were from VLa and VLp. Across cases, the projections from VLa were somewhat stronger, but more cells were labeled in VLp in case 03-74. The dorsal parts of these nuclei seem to be more densely connected to PMDc. Lateral VA (VApc) and VM project only sparsely to PMDc. IL and MDmf also provide substantial projections to PMDc.

Injections were placed in PMDr in three cases. The connections of PMDr resembled those of PMDc. In galago 01-98, an injection core of DY covered much of lateral PMDr, while also extending slightly into PMDc and adjoining prefrontal cortex (Fig. 9). Labeled neurons were concentrated in the rostral motor thalamus in VA, VLa and the rostral and medial parts of VLp (Fig. 16). The ventral extent of the cluster of labeled cells in VLp may have extended into VM. Other labeled neurons were in lateral MD (MDmf), and some were in IL. In cases 00-79 and 01-123, injection cores were restricted to PMDr (Fig. 9). The FE injections in these cases labeled fewer neurons than the DY injections in 01-98. In case 00-79, a focus of labeled cells in VA involved both VApc and VAmc. Only a few neurons were found in VLa and most rostral and medial parts of VLp. Some labeled neurons were found in lateral MD (Fig. 16). In case 01-123, the architectonic subdivisions of the motor thalamus were not as clear as in other cases. Thus, the indicated borders of the thalamic subdivisions are only approximate. Yet, as in other cases with PMDr injections, labeled cells were concentrated in the rostral motor thalamus including medial VA and VLp (Fig. 16). Some cells were in lateral MD, very few were in IL, and neurons in VLa were not labeled in case 01-123. Fewer labeled neurons were in VLp and VLa in cases with injections restricted to PMDr than in cases with injections in PMDc.

Thalamic Projections to PMV

Much of PMV represents orofacial movements (Wu et al., 2000; Fang et al., 2005). The thalamocortical connections of PMV were studied in four galagos with injections of tracers centered in the orofacial representation in PMV. The results were highly consistent across cases. In galago 03-65, an injection of BDA produced a small injection core centered in PMV (Fig. 9B). No other areas of cortex were involved. In horizontal sections through the thalamus, labeled neurons were concentrated in ventral and medial portions of VLa and VLp (Fig. 17-1). In this case, 70% of the labeled neurons were in VLp and 30% in VLa (Table 2). The distribution of labeled neurons was discontinuous, with separate foci in each nucleus. Labeled cells were only occasionally in VA. In addition to the motor thalamus, neurons were labeled in lateral MD (MDmf) and intralaminar nuclei (mostly CL).

In galago 00-79, a large injection core of FB in PMV (Fig. 9B) labeled a large number of thalamic neurons. In coronal sections, most of the labeled neurons were in VLp, VLa and some were in lateral VA, VApc (Fig. 17-2). Across all of these nuclei, the most medial and ventral part of the motor thalamus was mostly labeled. Only few labeled cells were located more laterally. The most ventral focus of labeled cells was assigned to VM, although the architectonic identification of VM was difficult in this case. Other labeled neurons were in IL and posterolateral MD. In case 01-39, an injection of WGA-HRP was confined to the center of PMV (Fig. 9B). In coronal sections, labeled neurons and terminals of corticothalamic projections were concentrated mostly in VLa and medial VLp (Fig. 17-2). Similar to case 00-79, the distribution of labeled neurons extended ventrally onto VM. Other labeled cells and terminals were in posterolateral MD and posterior IL. A very similar pattern was expressed in case 01-98 with a larger injection of WGA-HRP in PMV (not shown). Again, labeled cells were densely packed in the ventral and medial motor thalamus, with most of the labeled neurons in VLp and less in VLa. Other labeled neurons were in IL and posterolateral MD. Overall, the results indicate that the rostromedial sector of the motor thalamus projects to PMV, and that VLp and VLa provide most of these projections. VM, IL and posterolateral MD (MDmf) provided additional thalamic inputs.

Thalamic Projections to SMA

The thalamic connections of SMA were investigated in one galago in which a FR injection core was restricted to the forelimb representation (Fig. 9B). Most of the labeled neurons in the motor thalamus were in the central parts of VLa and VLp (Fig. 18). In this galago, more of the labeled neurons (58%) were in VLp, while somewhat fewer were in VLa (40%) (Table 2). The

most ventrally located labeled neurons were in VM. Outside the motor thalamus, a dense population of labeled neurons was in IL (mostly CL). Fewer labeled neurons were in CM and midline nuclei (MIN). Only a few labeled neurons were in MDmf, in contrast to the dense labeling in MDmf when injections were placed in adjoining PMD.

Thalamocortical Connections of the Frontal Eye Field (FEF)

Two galagos received tracer injections in the frontal eye field (FEF). In galago 00-79, an injection of FR was placed in the center of FEF and injection core was confined to the electrophysiologically defined FEF (Fig. 9B; Fang et al., 2005). Labeled neurons were anterior in the thalamus in VA nucleus involving its both parvo- and magnocellular subdivisions (Fig. 19-1). The distribution of labeled neurons extended somewhat into the anterior portion of medial VLp adjacent to IL, and into VM. Another focus of label was in IL and the lateral portion of MD. The results from another galago 01-39 (not shown) with FB injection in the FEF were similar. Most of the labeled neurons were in the ventral anterior thalamus, including VLa and VLp, and in the intralaminar nuclei. However, the total amount of labeled cells in case 01-39 was less than in case 00-79.

Thalamocortical Connections of Granular Frontal Cortex (Prefrontal Cortex)

Injections were placed just anterior to premotor areas and the FEF in two locations where electrical stimulation produced no movements. In galago 03-11, an injection of CTB was placed in cortex just anterior to PMDr (Fig. 9B). Labeled neurons were located ventromedially in motor thalamus, clustering mostly across the anteroposterior length of VM (Fig. 19-2). Other labeled neurons were in the most medial portion of VLp. Another focus of dense label was in the latero-central MD, corresponding to MDmf and MDpc. A few labeled neurons were also in the posterior IL (CL). Also in galago 03-11, an injection of BDA was placed in cortex just anterior to PMV. This injection also resulted in labeled neurons that were clustered in the ventromedial portion of the motor thalamus, mostly in VM, but also in medial VLp (Fig. 19-2). As for the more dorsal CTB injections, large numbers of labeled neurons were in the lateral (MDmf) and central (MDpc) portions of MD nucelus. Some labeled neurons were in IL. Together, these results suggest that the major projections to frontal cortex are from anterior and medial portions of the motor thalamus. The projections from MD to cortex anterior to PMDr, and especially cortex anterior to PMV, were very dense. In the one FEF case, MD was also the major source of projections to FEF.

DISCUSSION

In this study, thalamic neurons projecting to five motor areas of frontal cortex and locations in adjoining prefrontal cortex of galagos were labeled by injections of tracers into cortex. An architectonic study of the thalamus allowed us to define and characterize relevant motor and other nuclei, and labeled neurons were localized within architectonic subdivisions of the thalamus. The results are discussed in two parts. First, the results of the architectonic study of the motor thalamus are compared to previous depictions of thalamic organization in prosimian and simian primates. Next, the thalamic connection patterns of motor and premotor areas of cortex in galagos are related to the results of the few previous studies of thalamic connections in galagos, and then to the more extensive studies on simian primates, especially the well-studied macaque monkeys. Finally, we summarize the main conclusions stemming from this study.

Subdivisions of the Motor and Adjoining Thalamus in Galagos and Other Primates

Our architectonic study was directed toward identifying subdivisions of the motor thalamus of galagos. The motor thalamus and adjoining parts of the thalamus have been subdivided and named in various ways by previous investigators (see Macchi and Jones, 1997, for review),

but for monkeys, a general consensus is starting to emerge. There is general agreement that three major subdivisions of the motor thalamus exist in macaque monkeys, a ventral anterior region (VA), a ventral medial region (VM), and a ventrolateral region (VL). VA is further divided into magnocellular (VAmc) and parvocellular (VApc) subnuclei. VL is further divided into an anterior nucleus (VLa) with pallidal inputs and a posterior region (VLp) with cerebellar inputs, and VLp is further divided into three regions or nuclei (Table 3). Some of the terms for thalamic subdivisions have been retained from the influential atlas of Olszewski (1952), but current terms largely come from those used by Jones (1985). Stepniewska et al. (1994a) identified these subdivisions of the motor thalamus in New World owl monkeys. Here we extend this nomenclature to prosimian galagos in an effort to identify regions in the thalamus that are homologous to those portrayed in New and Old World monkeys. Part of the argument for the identity of homologous regions stems from similarities in relative position and in architectonic characteristics, as discussed below. The important evidence of similarities in subcortical inputs is unfortunately missing, as the territories of inputs from the cerebellar nuclei, and the pallidum (Sakai et al., 1996; 1999; 2000; 2002) have not yet been determined in galagos. However, the projections of thalamic regions and nuclei to subdivisions of motor cortex were determined for galagos in the present study, and comparisons with monkeys provide further evidence, as discussed below, for the identities of the proposed subdivisions of the motor thalamus.

Architectonic Subdivisions of the Motor Thalamus in Galagos

In the present study, it soon became obvious that subdivisions of the motor thalamus were not as clearly differentiated in galagos as in the more thoroughly studied macaque monkeys and several taxa of New World monkeys. Earlier studies of the architecture of the thalamus in prosimian primates, most notably those of Clark (1932), Kanagasuntheram et al. (1968), Simmons (1980) and Jones (1985), were largely restricted to considering only Nissl and sometimes myelin-stained sections, and usually a single plane of section. Here we studied sections stained for Nissl substance and myelin, but also sections processed for CO, AChE, the Cat 301 antigen, Cb, and Pv. In addition, sections cut in the coronal (frontal), sagittal, and horizontal planes were examined. Across these procedures and cutting planes, horizontal sections stained for AChE presented the most clear and consistent results across cases. Nevertheless, we had difficulties in identifying some of the boundaries and subdivisions now commonly recognized in monkeys.

To briefly summarize the architectonic results, a large ventral lateral (VL) region occupies about two-thirds of the motor thalamus in galagos. Within VL, a smaller anterior (VLa) division and a larger posterior (VLp) division are easily distinguished. In AChE, CO, and Pv preparations, VLp can be recognized as a darkly stained structure. In particular, VLp had a dark reticular pattern that appears to reflect the presence of the AChE enzyme in the endothelial cells of the walls of the capillaries of blood vessels. VLp is also characterized by a scattering of AChE-stained cell bodies, and an AChE-dense neuropil. The expression of AChE is uneven in VLp, being denser in medial VLp, suggesting the possibility of functional subdivisions. In Nissl stained sections, VLp is a region of densely packed cells, with more differences in cell size, shape and packing across the structure. These architectonic differences between lateral, middle and medial parts of VLp likely relate to the slightly different functions of these parts of VLp, as the lateral, middle and medial regions project to sectors of M1 successively representing the trunk, forelimb, or mouth and face (Fig. 21).

The reasons for the modification of the capillary system throughout VLp of galagos are unclear. Such an AChE positive system of capillaries has not been reported for VLp of monkeys. However, the existence of such a modification in the capillary system throughout a functional subdivision of the brain is not surprising, given the close association between levels of

metabolic activity and blood flow. Nevertheless, the reasons for high AChE levels in capillaries in VLp of galagos, and perhaps other prosimian primates, is presently unknown (see Stepniewska et al., 1994a for discussion).

The anterior division of the VL complex, VLa, is characterized in AChE preparations by darkly stained cell bodies and a lightly stained neuropil. VLa is difficult to distinguish in other preparations, but neurons appear to be smaller and more densely packed than the neurons in VLp in Nissl preparations. As described in monkeys (Jones, 1985;1998;Stepniewska et al., 1994a), cells in VLa tend to be grouped in clusters. In galagos, Jones (1985) distinguished a VL region in coronal Nissl sections, and later identified anterior (VLa) and posterior (VLp) divisions (Jones, 1998). In a myelin stained section, Simmons (1980) identified VL in the relative position of the present VLp. In our preparations, the myelin staining of VLp was not much different from that of VLa. However, in favorable sections, VLa can be distinguished by bundles of darkly stained fibers that are packed more densely than in VLp. Finally, in coronal Nissl sections, Kanagasuntheram et al. (1968) described a ventral anterior (VA) and a ventral lateral (VL) nucleus, and these divisions include the present VA, VL, and VM regions.

In owl monkeys (Stepniewska et al., 1994a) and macaque monkeys (Olszewski, 1952), VLa contains mostly small cells that are clustered in small groups, as in galagos. However, VLa of owl monkeys is characterized by a pattern of darkly stained capillaries in AChE preparations (Stepniewska et al., 1994a), whereas a darkly stained capillary network was found in VLp, rather than VLa, in galagos. As VLa is anterior to VLp in galagos and monkeys, it is unlikely that these regions have been misidentified in galagos. Rather, it appears that an AChE-positive network has emerged in different parts of VL in galagos and owl monkeys. Neither region has a comparable AChE-positive capillary network in macaques (Stepniewska et al., 2003). In macaque monkeys, VLa is very dark in calbindin preparations, while VLp is quite light and the adjoining VA is moderately dark (Stepniewska et al., 2003). In macaque monkeys, VLa contains many parvalbumin and calbindin positive neurons (see Jones, 1998a,b), but this was not noted in galagos. However, in both macaques (Jones, 1998a,b) and galagos, VLp has many parvalbumin positive cells. In galagos, VLp is rather homogeneous in appearance across preparations, with only a weak tendency for cells in medial VLp to be larger than those are elsewhere. In contrast, VLp has been divided into three variously named nuclei or regions in both macaques and owl monkeys (Table 3). The medial area X in macaques and VLx in owl monkeys is most obvious as a region of large, evenly distributed cells in comparison with the even larger, darker in Nissl, and unevenly distributed neurons in VLp. Thus, VLp is not as differentiated architectonically in galagos as in simians, although functionally distinct divisions may exist, as connection patterns suggest (see below).

The smaller ventral anterior region, VA, of galagos is the most anterior part of the motor thalamus. In horizontal brain sections processed for AChE, VA is lighter than VLp, but darker than VLa. A lateral part of VA, VApc, is distinguished from a medial part, VAmc, by a darkly stained capillary network that is considerably less dense than the capillary network in VLp. VAmc differs from VApc in having a number of AChE positive cell bodies. In Nissl preparations, cells in VA are clustered, but the clusters are smaller in VApc than in VAmc. VApc and VAmc correspond to the parvocellular (VApc) and magnocellular (VAmc) divisions of VA in monkeys (Table 3). VA, as defined here, appears to approximate the region denoted as VA in galagos by Jones (1985) and by Simmons (1980) in other prosimians. In macaques, VA is lighter in Cat 301 and Cb preparations and darker in AChE preparations than adjoining VLa (Stepniewska et al., 2003).

The ventral medial, VM, region is a subdivision of the motor thalamus that is just ventral to VLa, posterior to VA, and anterior to VLp. In AChE preparations, VM is much lighter than adjacent structures. In both CO and Pv preparations, VM is lightly-to-moderately stained. In

Nissl sections, VM has lighter stained cells than VLa and VLp. No subdivisions of VM were apparent. Previously, Simmons (1980) described VM of prosimians as poorly differentiated from VA. In macaques, VM has been considered to be a medial subdivision of the VL complex, or as a separate nucleus or complex, VM (Table 3). In owl monkeys, VM is not well differentiated from the adjacent thalamus in AChE or CO preparations (Stepniewska et al., 1994a).

Other thalamic nuclei that have connections with frontal cortex in galagos include the anterior and posterior nuclei (Pc, CL, and CM) of the intralaminar (IL) complex, and the multiform (MDmf), parvocellular (MDpc), and magnocellular (MDmc) divisions of the medial dorsal nucleus. Some of these subdivisions have been distinguished in Nissl and fiber stained coronal sections in galagos by Kanagasutheram et al. (1968) and Jones (1985), and in other prosimians by Simmons (1980). The basic architectonic features that distinguish these nuclei are very similar in galagos and monkeys (e.g., Olszewski, 1952;Jones, 1985;Stepniewska et al., 1994a). However, there are some differences. In MD, MDpc is darkly stained in AChE preparations in galagos, but lightly-to-moderately stained in monkeys, while MDmf is moderately stained in galagos, but darkly stained in monkeys (Stepniewska et al., 1994a). Such differences in staining suggest that the functions of these nuclei differ slightly in galagos and monkeys.

Thalamic Connections of Motor Areas and Prefrontal Cortex

In the present study, we determined how labeled neurons were distributed in the thalamus after injections in different motor areas of galagos. In addition, the projections from the motor thalamus to different parts of the body representation in primary motor cortex, M1, were determined. The overall pattern of thalamic projections to the four major motor areas (PMD, PMV, SMA, and M1) is summarized in figure 20. Thus, in galagos, VLp provided dense inputs into M1, PMV, caudal PMD (PMDc), and SMA (Table 2). The posterior part of VLp was more densely connected with M1 and PMV, while the anterior part of VLp was more connected with PMD and SMA. Most of the other motor cortex connections of the thalamus were from VLa, which projected more to PMDc than to M1, PMV and SMA. VM had some connections with PMV and PMD, while VApc had dense projections only to PMD (mostly rostral-PMDr), and very sparse projections to other motor regions. Thus, as in macaques (Macchi and Jones, 1997), VLp and VLa provide the majority of the projections to motor cortex, and VM and VA provide so few that they barely qualify as motor nuclei. Given the uncertainty of some of the borders of these nuclei in the present experimental material, quite possibly some of the labeled neurons judged to be in VM and VA were in VLa or VLp.

In addition to these projections from motor thalamus, the motor-related intralaminar nuclei and medial dorsal nucleus projected to motor cortex. Most notably, MDmf projected densely to both PMD and PMV, but not to M1. CM sent some projections to SMA and M1, and IL had significant pojection to all motor regions. Finally, neurons in the anterior pulvinar were labeled by some of the injections in motor cortex, suggesting that this nucleus provides some inputs. In newborn, but not adult macaques, the anterior pulvinar projects extemsively to frontal motor areas (Darian-Smith et al., 1990).

Major features of the topographic patterns of projections of the motor thalamus to motor cortex are shown in figure 21. A lateral portion of VLp projects to the trunk and hindlimb sector of M1, a more medial portion to the forelimb sector, and a medial portion to the orofacial sector. This pattern continues into the posterior part of histologically defined VLa. A possible interpretation of this result is that the connection pattern more accurately reflects the border between VLa and VLp, than the architectonic pattern, and only VLp projects to M1. Here we have based thalamic borders on architectonic differences, while recognizing that such borders are sometimes difficult to distinguish. As another topographic feature, the forelimb portions

of M1, PMD, and SMA have connections with different parts of the motor thalamus even though the same body part was involved in each area. Projections to the forelimb representation of M1, SMA, and PMD involved successively more anterior portions of the motor thalamus, mainly in VLp and VLa, but also in VM.

In general, the patterns of thalamocortical motor connections reported for macaques (e.g., Jones et al., 1979; Schell and Strick, 1984; Darian-Smith et al., 1990; Nakano et al., 1993; Shindo et al., 1995; Matelli and Luppino, 1996; Rouiller et al., 1999; Morel et al., 2005) are similar to those reported here for galagos. In both macaques and galagos, M1 receives dense inputs from VLp, less dense inputs from VLa, and only a few inputs from VM and VA. PMV receives dense inputs from medial VLp (area X), and less dense inputs from VLa, VM and MDmf. Similar projections to M1 have been reported for New World owl monkeys (Stepniewska et al., 1994b). PMD in galagos has connections that resemble those of PMDc and PMDr combined in macaques. Thus, connections were mainly with VLa and anterior VLp and MDmf. In galagos, SMA connections were investigated in only one case, and major inputs were from VLa and VLp. In macaques, inputs to SMA are dense from VLa and VLp, while a notable projection comes from MD (e.g. Matelli and Luppino, 1996), which was not seen in galagos.

Finally, an injection into the physiologically-defined frontal eye field (FEF) labeled neurons in VA, VLp, lateral MD (possible MDmf) and IL. These thalamic projection zones correspond to those reported for New and Old World monkeys after injections in the FEF (Huerta et al., 1986). In one galago, different tracers were injected into granular frontal cortex just anterior to PMD and PMV. Each injection labeled neurons largely in VA and MD. In simian primates, major thalamic projections to prefrontal cortex originate in MD, and other notable projections come from VA (see Fuster, 1988 for review; Tobias, 1975; Goldman-Rakic and Porrino, 1985; Russchen et al., 1987; Bachevalier et al., 1997; Erikson et al., 2004).

CONCLUSIONS

The present results support a number of conclusions. First, our histological study of the thalamus allowed us to identify the major nuclei of the motor thalamus in galagos. By using a battery of histological procedures and three planes of section, VLa, VLp, VApc, VAmc, and VM nuclei were identified, and these structures appear to closely correspond to subdivisions of the thalamus in simian primates. In addition, the associated intralaminar nuclei, anterior: Pc and CL, and posterior: CM and Pf, as well as the mediodorsal nucleus, MD, with magnocellular (MDmc), parvocellular (MDpc), and multiform (MDmf) divisions have been identified as similar to those structures in other primates. Thus, there appears to be a similar pattern of differentiated motor nuclei in the thalamus of both prosimians and anthropoids. Second, these thalamic nuclei are less histologically distinct in galagos than in monkeys. Thus, precise borders can be difficult to demarcate in some planes of section. Third, thalamic connection patterns with motor, premotor, and supplementary motor areas of cortex indicate that VLa and VLp are the principal motor nuclei, with VLp contributing dense inputs to M1, but also to PMV, PMD, and SMA. VLa projects moderately to M1 and SMA, while projecting densely to PMD. VLa and VLp are also considered to be the major motor structures of the thalamus in monkeys. In monkeys, VLp is further distinguished by receiving most of the cerebellar inputs, while VLa is dominated by pallidal inputs (e.g. Schell and Strick, 1984; Sakai et al., 1996, 2002). The distributions of cerebellar and pallidal inputs to the thalamus in galagos are not yet known. Determining the distribution of each input could help define VLp and VLa in galagos. Fourth, the other two regions of the presumptive motor thalamus, VM and VA, have only minor connections with areas of motor cortex, and their main functions may not be motor. These nuclei have connections with prefrontal cortex, FEF and pre-SMA in monkeys (Kunzle and Akert, 1977; Goldman-Rakic and Porrino, 1985; Ilinsky et al., 1985; Morel et al., 2005), and

our injections in prefrontal cortex of galagos labeled these nuclei. In monkeys, projections from the substantia nigra to VA and VM (Macchi and Jones, 1997) implicate these nuclei in motor functions, although direct projections from VAmc and VM to motor areas of cortex in macaques are sparse. Fifth, each of the four motor areas investigated in this study (SMA, PMD, PMV and M1) has a unique pattern of connections with motor, intralaminar, and mediodorsal nuclei, reinforcing the conclusion based on cortical mapping with microstimulation, cortical architecture, and cortical connection patterns, that these fields constitute functionally distinct divisions of motor cortex in galagos that have homologues in anthropoid primates.

LIST OF ABBREVIATION

Motor Thalamus (MoT)

VA
: Ventral anterior nucleus

VApc
: Ventral anterior nucleus, lateral (parvocellular) subdivision

VAmc
: Ventral anterior nucleus, medial (magnocellular) subdivision

VAp
: Ventral anterior nucleus, principal division

VL
: Ventral lateral nucleus

VLa
: Ventral lateral nucleus, anterior subdivision

VLc
: Ventral lateral nucleus, pars caudalis

VLm
: Ventral lateral nucleus, medial division

VLo
: Ventral lateral nucleus, pars oralis

VLp
: Ventral lateral nucleus, posterior subdivision

VM
: Ventral medial nucleus

VPLo
: Ventroposterior lateral nucleus, pars oralis

Intralaminar Nuclei (IL)

CL
: Central lateral nucleus

CM
: Centromedian nucleus

Pc

Paracentral nucleus

Pf
Parafascicular nucleus

Medial Dorsal Nucleus (MD)

MDmf
Medial dorsal nucleus, multiform subdivision

MDpc
Medial dorsal nucleus, parvocellular subdivision

MDmc
Medial dorsal nucleus, magnocellular subdivision

Other Thalamic Nuclei

ANT
Anterior nuclei

PA
Pulvinar, anterior subdivision

BG
Basal ganglia

Hb
Habenular nucleus

IC
Internal capsule

LD
Lateral dorsal nucleus

LGN
Lateral geniculate nucleus

LP
Lateral posterior nucleus

MGN
Medial geniculate nucleus

MIN
Midline nuclei

mtt
Mammillothalamic tract

Pul
Pulvinar

Rt
Reticular nucleus

SC
Superior colliculus

VP
: Ventral posterior nucleus

Cortical Areas and structures

FSa
: Frontal sulcus, anterior

FSp
: Frontal sulcus, posterior

M1
: Primary motor area

PMD
: Dorsal premotor cortex

PMV
: Ventral premotor cortex

SMA
: Supplementary motor area

FEF
: Frontal eye field

PFC
: Prefrontal cortex

Movements

Tk/HL
: Trunk and hindlimb movements

OF
: Orofacial movements

EM
: Eye movements

Mix
: Shoulder, trunk, neck, ear, eyelid and eye movements

Anatomical tracers

BDA
: biotinylated dextran amine

CTB
: cholera toxin subunit B

WGA-HRP
: wheat-germ agglutinin conjugated to horseradish peroxidase

DY
: diamidino yellow

FB
: fast blue

FE

fluoroemerald

FR

fluororuby

REFERENCES

Bachevalier J, Meunier M, Lu MX, Ungerleider LG. Thalamic and temporal cortex input to medial prefrontal cortex in rhesus monkeys. Exp Brain Res 1997;15:430–444. [PubMed: 9262198]

Bruce K, Grofova I. Notes on a light and electron microscopic double-labeling method combining anterograde tracing with Phaseolus vulgaris leucoagglutinin and retrograde tracing with cholera toxin subunit B. J Neurosci Methods 1992;45:23–33. [PubMed: 1283431]

Celio MR. Calbindin D-28k and parvalbumin in the rat nervous system. Neuroscience 1990;35:375–475. [PubMed: 2199841]

Clark WEL. The structure and connections of the thalamus. Brain 1932;55:406–470.

Collins CE, Stepniewska I, Kaas JH. Topographic patterns of V2 cortical connections in a prosimian primate (*Galago garnetti*). J Comp Neurol 2001;431:155–167. [PubMed: 11169997]

Darian-Smith I, Cheema SS, Darian-Smith C. Thalamic projections to sensorimotor cortex in the newborn macaque. J Comp Neurol 1990;299:17–46. [PubMed: 1698837]

Erickson SL, Melchitzky DS, Lewis DA. Subcortical afferents to the lateral mediodorsal thalamus in cynomolgus monkeys. Neuroscience 2004;129:675–690. [PubMed: 15541889]

Fang P-C, Stepniewska I, Kaas JH. Ipsilateral cortical connections of motor, premotor, frontal eye, and posterior parietal fields in a prosimian primate, *Otolemur garnetti*. J Comp Neurol 2005;490:305–333. [PubMed: 16082679]

Fleagle, JG. Primate Adaptation and Evolution. 2nd edn. Academic Press; San Diego: 1999.

Fuster, JM. The Prefrontal Cortex. 2nd edn. Raven Press; New York: 1988.

Gallyas F. Silver staining of myelin by means of physical development. Neurol Res 1979;1:203–209. [PubMed: 95356]

Geneser-Jensen FA, Blackstad TW. Distribution of acetyl cholinesterase in the hippocampal region of the guinea pig. I. Entorhinal area, parasubiculum, and presubiculum. Z Zellforsch Mikrosk Anat 1971;114:460–481. [PubMed: 5550728]

Gibson AR, Hansma DI, Houk JC, Robinson FR. A sensitive low artifact TMB procedure for the demonstration of WGA-HRP in the CNS. Brain Res 1984;298:235–241. [PubMed: 6202368]

Goldman-Rakic PS, Porrino LJ. The primate mediodorsal (MD) nucleus and its projection to the frontal lobe. J Comp Neurol 1985;242:535–560. [PubMed: 2418080]

Hockfield S, McKay RD, Hendry SH, Jones EG. A surface antigen that identifies ocular dominance columns in the visual cortex and laminar features of the lateral geniculate nucleus. Cold Spring Harb Symp Quant Biol 1983;48:877–889. [PubMed: 6426850]

Huerta MF, Krubitzer LA, Kaas JH. Frontal eye field as defined by intracortical microstimulation in squirrel monkeys, owl monkeys, and macaque monkeys: I. Subcortical connections. J Comp Neurol 1986;253:415–439. [PubMed: 3793998]

Ilinsky IA, Jouandet ML, Goldman-Rakic PS. Organization of the nigrothalamocortical system in the rhesus monkey. J Comp Neurol 1985;236:315–330. [PubMed: 4056098]

Jones EG, Coulter JD, Wise SP. Commissural columns in the sensory-motor cortex of monkeys: Differential thalamic relationships of sensory-motor and parietal cortical fields in monkeys. J Comp Neurol 1979;188:113–135. [PubMed: 115905]

Jones, EG. Plenum Press; New York and London: 1985. The Thalamus.

Jones EG. Viewpoint: the core and matrix of thalamic organization. Neuroscience 1998a;85:331–345. [PubMed: 9622234]

Jones, EG. Thalamus of primates. In: Bloom, FE.; Bjorklung, A.; Hokfelt, T., editors. Handbook of chemical neuroanatomy. Elsevier: 1998b. p. 1-298.

Jones EG. The thalamic matrix and thalamocortical synchrony. Trends Neurosci 2001;24:595–601. [PubMed: 11576674]

Kaas JH, Huerta MF, Weber JT, Harting JK. Patterns of retinal terminations and laminar organization of the lateral geniculate nucleus of primates. J Comp Neurol 1978;182:517–553. [PubMed: 102662]

Kaas JH. Evolution of somatosensory and motor cortex in primates. Anat Rec 2004;281A:1148–1156.

Kanagasuntheram R, Wong WC, Krishnamurti A. Nuclear configuration of the diencephalon in some lorisoids. J Comp Neurol 1968;133:241–268. [PubMed: 5680004]

Krubitzer LA, Kaas JH. The organization and connections of somatosensory cortex in marmosets. J Neurosci 1990;10:952–974. [PubMed: 2108231]

Kunzle H, Akert K. Efferent connections of cortical, area 8 (frontal eye field) in Macaca fascicularis. A reinvestigation using the autoradiographic technique. J Comp Neurol 1977;173:147–164. [PubMed: 403205]

Lyon DC, Kaas JH. Connectional evidence for dorsal and ventral V3, and other extrastriate areas in the prosimian primate, Galago garnetti. Brain Behav Evol 2002;59:114–129. [PubMed: 12119531]

Macchi G, Jones EG. Toward an agreement on terminology of nuclear and subnuclear divisions of the motor thalamus. J Neurosurg 1997;86:670–685. [PubMed: 9120632]

Martin RD. Palaeontology: Chinese lantern for early primates. Nature 2004;427:22–23. [PubMed: 14702069]

Matelli M, Luppino G. Thalamic input to mesial and superior area 6 in the macaque monkey. J Comp Neurol 1996;372:59–87. [PubMed: 8841922]

Morel A, Liu J, Wannier T, Jeanmonod D, Rouiller EM. Divergence and convergence of thalamocortical projections to premotor and supplementary motor cortex: a multiple tracing study in the macaque monkey. Eur J Neurosci 2005;21:1007–1029. [PubMed: 15787707]

Nakano K, Hasegawa Y, Kayahara T, Tokushige A, Kuga Y. Cortical connections of the motor thalamic nuclei in the Japanese monkey, Macaca fuscata. Stereotact Funct Neurosurg 1993;60:42–61. [PubMed: 7685538]

Olszewski, J. An Atlas for Use with the Stereotaxic Instrument. Karger; Basel: 1952. The Thalamus of Macaca Mulatta.

Preuss TM, Goldman-Rakic PS. Myelo- and cytoarchitecture of the granular frontal cortex and surrounding regions in the strepsirhine primate Galago and the anthropoid primate Macaca. J Comp Neurol 1991;310:429–474. [PubMed: 1939732]

Rouiller EM, Tanne J, Moret V, Boussaoud D. Origin of thalamic inputs to the primary, premotor, and supplementary motor cortical areas and to area 46 in macaque monkeys: A multiple retrograde tracing study. J Comp Neurol 1999;409:131–152. [PubMed: 10363716]

Rowe, N. The Pictorial Guide to the Living Primates. Pogonias Press; New York: 1996.

Russchen FT, Amaral DG, Price JL. The afferent input to the magnocellular division of the mediodorsal thalamic nucleus in the monkey, Macaca fascicularis. J Comp Neurol 1987;256:175–210. [PubMed: 3549796]

Sakai ST, Inase M, Tanji J. Comparison of cerebellothalamic and pallidothalamic projections in the monkey (Macaca fuscata): a double anterograde labeling study. J Comp Neurol 1996;368:215–228. [PubMed: 8725303]

Sakai ST, Inase M, Tanji J. Pallidal and cerebellar inputs to thalamocortical neurons projecting to the supplementary motor area in Macaca fuscata: a triple-labeling light microscopic study. Anat Embryol (Berl) 1999;199:9–19. [PubMed: 9924930]

Sakai ST, Stepniewska I, Qi HX, Kaas JH. Pallidal and cerebellar afferents to pre-supplementary motor area thalamocortical neurons in the owl monkey: A multiple labeling study. J Comp Neurol 2000;417:164–180. [PubMed: 10660895]

Sakai ST, Inase M, Tanji J. The relationship between MI and SMA afferents and cerebellar and pallidal efferents in the macaque monkey. Somatosens Mot Res 2002;19:139–148. [PubMed: 12088388]

Schell GR, Strick PL. The origin of thalamic inputs to the arcuate premotor and supplementary motor areas. J Neurosci 1984;4:539–560. [PubMed: 6199485]

Shindo K, Shima K, Tanji J. Spatial distribution of thalamic projections to the supplementary motor area and the primary motor cortex: a retrograde multiple labeling study in the macaque monkey. J Comp Neurol 1995;357:98–116. [PubMed: 7673471]

Simmons RM. The morphology of the diencephalon in the Prosimii. II. The Lemuroidea and Lorisoidea. Part I. Thalamus and metathalamus. J Hirnforsch 1980;21:449–491. [PubMed: 7451944]

Stepniewska I, Preuss TM, Kaas JH. Architectonic subdivisions of the motor thalamus of owl monkeys: Nissl, acetylcholinesterase, and cytochrome oxidase patterns. J Comp Neurol 1994a;349:536–557. [PubMed: 7860788]

Stepniewska I, Preuss TM, Kaas JH. Thalamic connections of the primary motor cortex (M1) of owl monkey. J Comp Neurol 1994b;349:558–582. [PubMed: 7532193]

Stepniewska I, Sakai ST, Qi HX, Kaas JH. Somatosensory input to the ventrolateral thalamic region in the macaque monkey: potential substrate for parkinsonian tremor. J Comp Neurol 2003;455:378–395. [PubMed: 12483689]

Tobias TJ. Afferents to prefrontal cortex from the thalamic mediodorsal nucleus in the rhesus monkey. Brain Res 1975;83:191–212. [PubMed: 1109293]

Veenman CL, Reiner A, Honig MG. Biotinylated dextran amine as an anterograde tracer for single- and double-labeling studies. J Neurosci Methods 1992;41:239–254. [PubMed: 1381034]

Wong-Riley M. Changes in the visual system of monocularly sutured or enucleated cats demonstrable with cytochrome oxidase histochemistry. Brain Res 1979;171:11–28. [PubMed: 223730]

Wu CW, Bichot NP, Kaas JH. Converging evidence from microstimulation, architecture, and connections for multiple motor areas in the frontal and cingulate cortex of prosimian primates. J Comp Neurol 2000;423:140–177. [PubMed: 10861543]

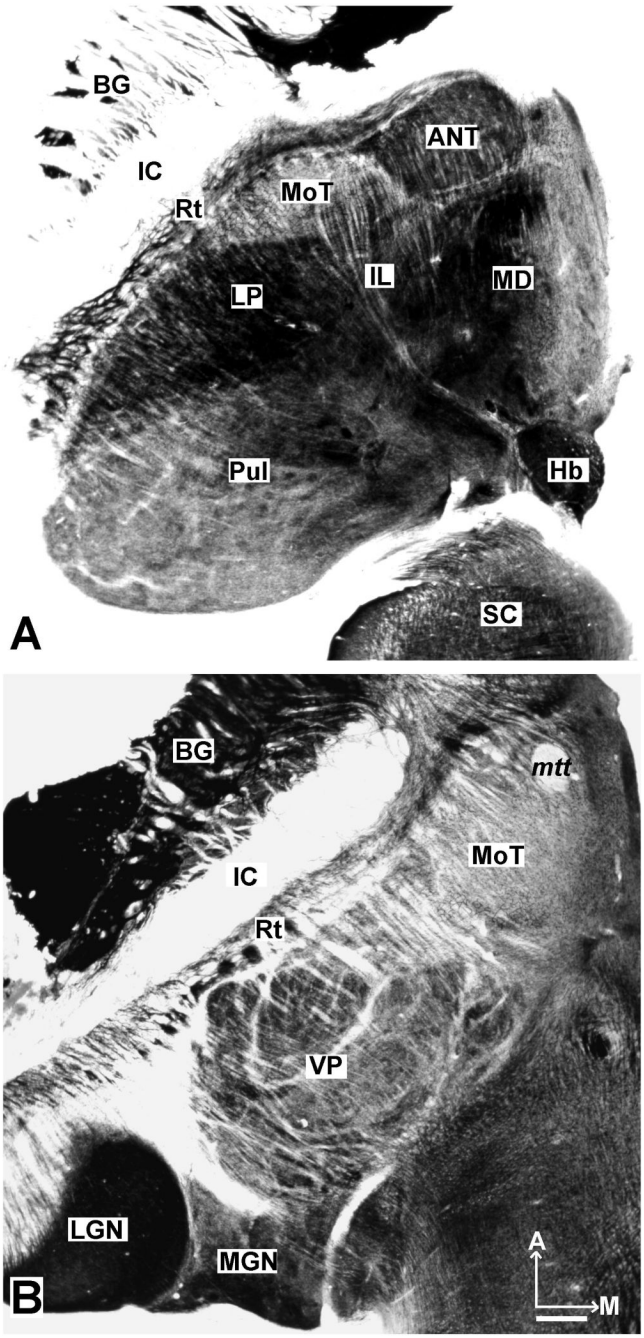

Fig 1.

The thalamus of a galago (#03-74) in horizontal sections processed for AChE. **A**. A more dorsal section through the thalamus locates the motor thalamus (MoT) just anterior to the lateral posterior (LP) and intralaminar (IL) nuclear, lateral to the anterior nucleus (ANT), and medial and posterior to the reticular nucleus (Rt). The medial dorsal (MD) nucleus, habenular (Hb), pulvinar complex (Pul), and superior colliculus (SC) are shown for reference. **B**. At a more ventral level, the motor thalamus occupies more of the anterior region. The larger ventroposterior nucleus (VP), just posterior to the motor thalamus, is subdivided by poorly stained septa. Other structures include the lateral geniculate nucleus (LGN), the medial geniculate nucleus (MGN), the reticular nucleus (Rt), the mammillothalamic tract (mtt), the

internal capsule (IC), and the globus pallidus (GP). Scale bar = 1mm. Sections are 2.25 mm apart.

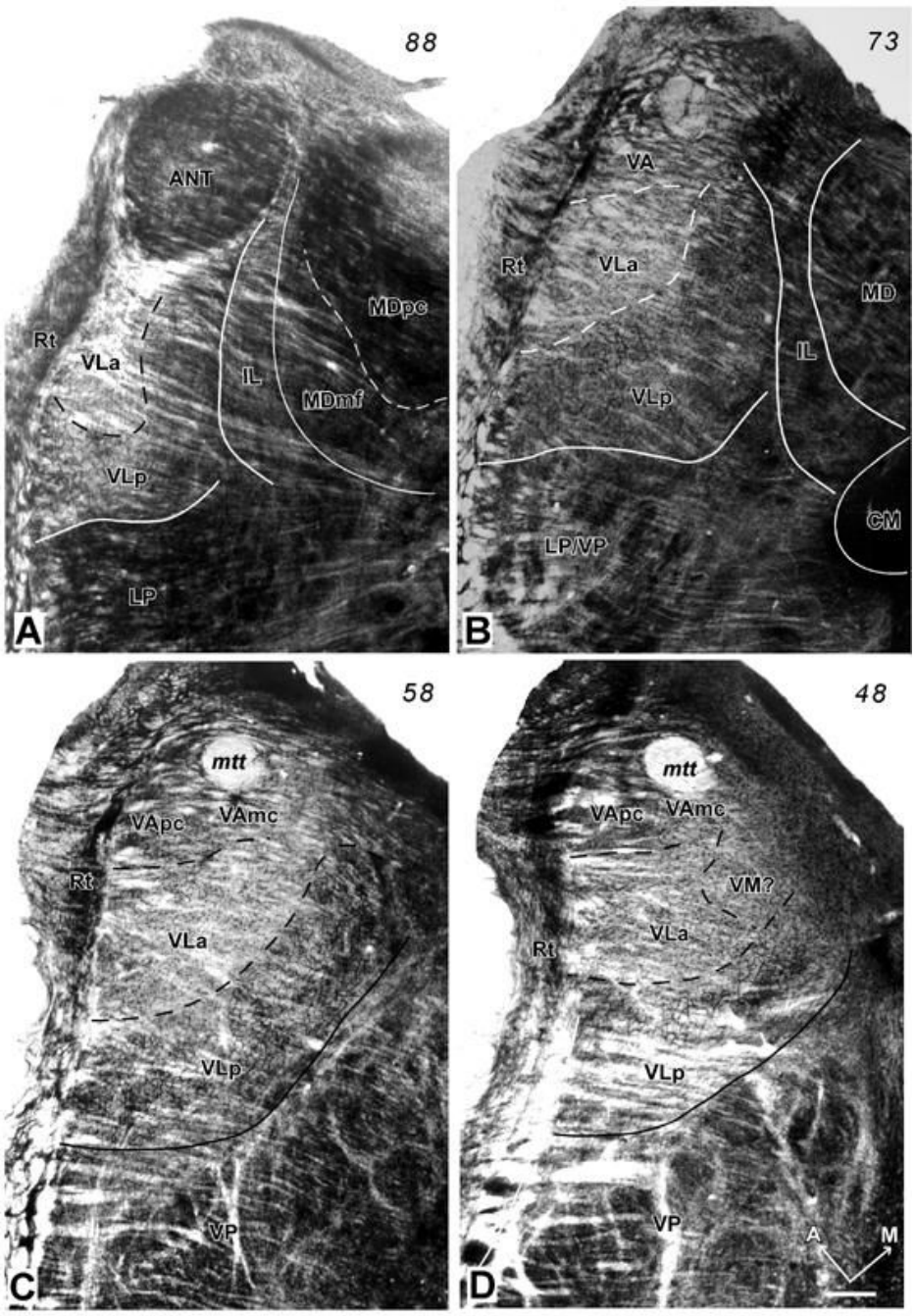

Fig 2.

Photomicrographs of AChE stained sections through the motor thalamus of a galago (#03-74). The thalamus was sectioned horizontally from dorsal (**A**) to ventral (**D**). The distance between A and B, and B and C is 600μm and between C and D is 400μm. The major subdivisions of the motor thalamus (VA, VL and VM) are identified. The densely-packed capillary network in VLp provides the most striking landmark of the motor thalamus. The solid lines are the boundaries of the motor thalamus, and the dashed lines are the approximated borders of subdivisions of the motor thalamus. A = anterior; M = medial; Scale bar = 0.5mm. See p2~p4 for abbreviations.

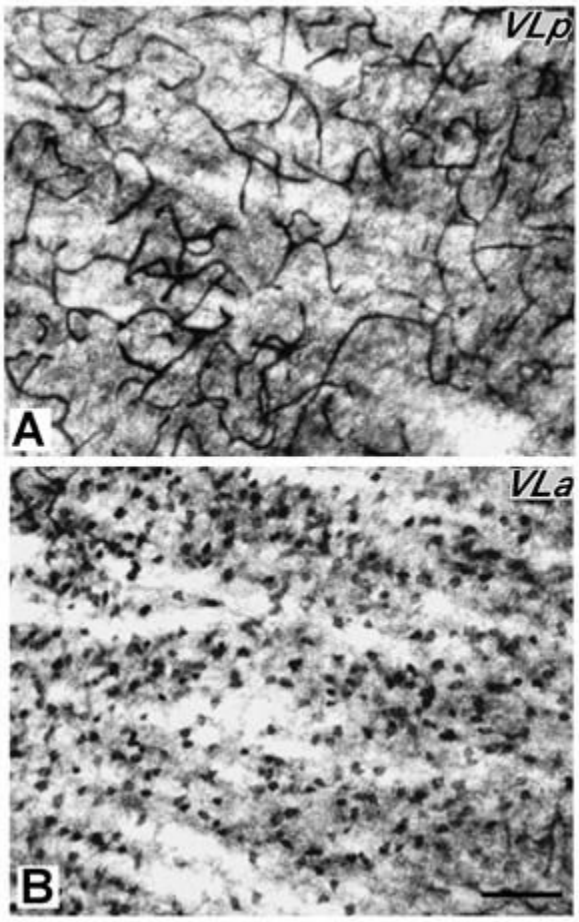

Fig 3.

Higher magnification photomicrographs of a AChE-stained section (section C of figure 2). **A**. VLp is densely-packed with darkly-stained capillaries. **B**. VLa is densely-packed with densely-stained with AChE positive cell bodies. Scale bar = 250 μm.

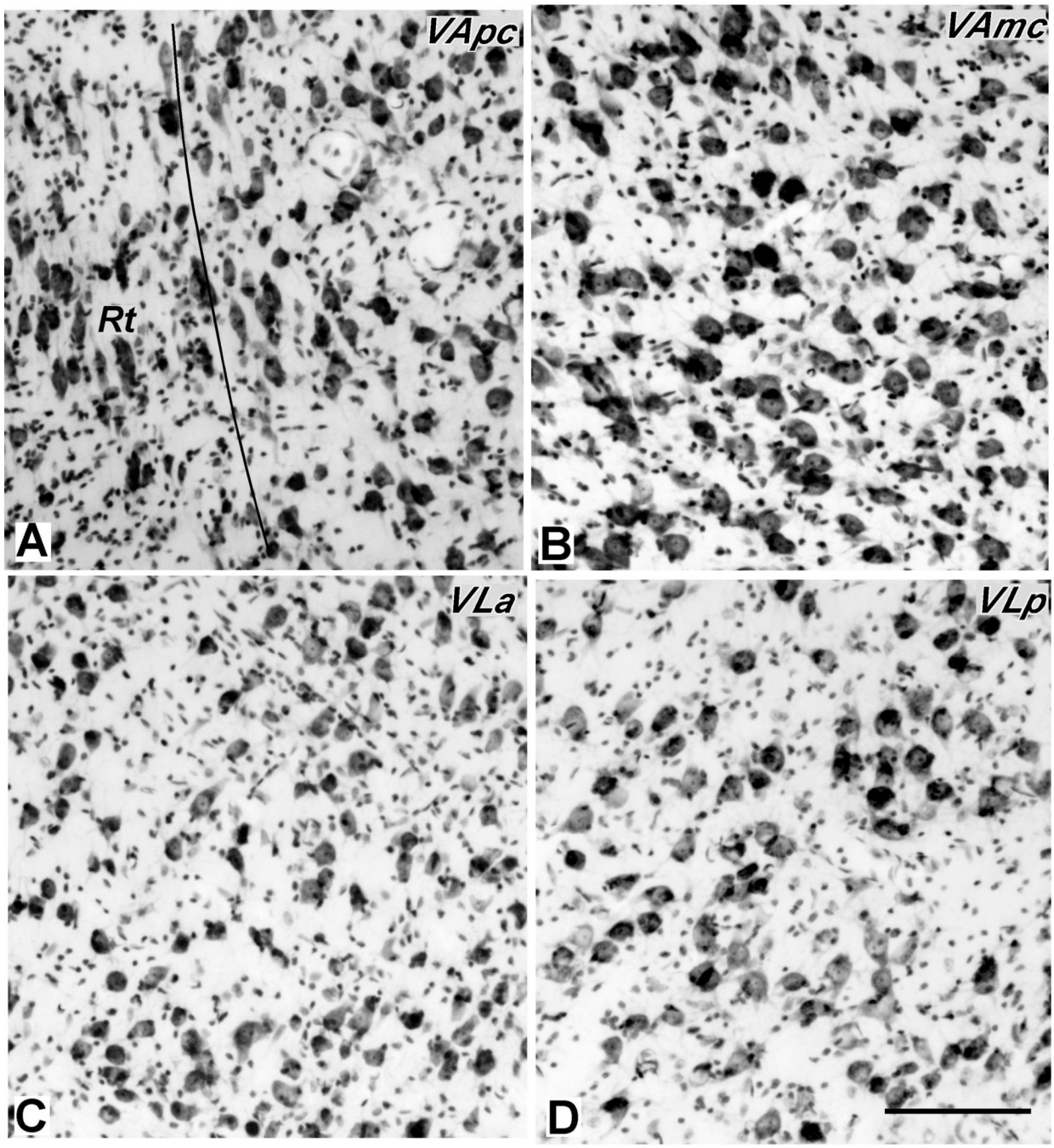

Fig 4.

Photomicrographs of Nissl-stained sections through the motor thalamus of galago 03-19 at high magnification showing the cells in the VApc (A) and VAmc (B) of ventral anterior thalamus, and VLa (C) and VLp (D) of ventral lateral thalamus. The cells in VAmc are larger than in VApc, and cells in VLp are larger than those in VLa. Scale bar = 250 μm.

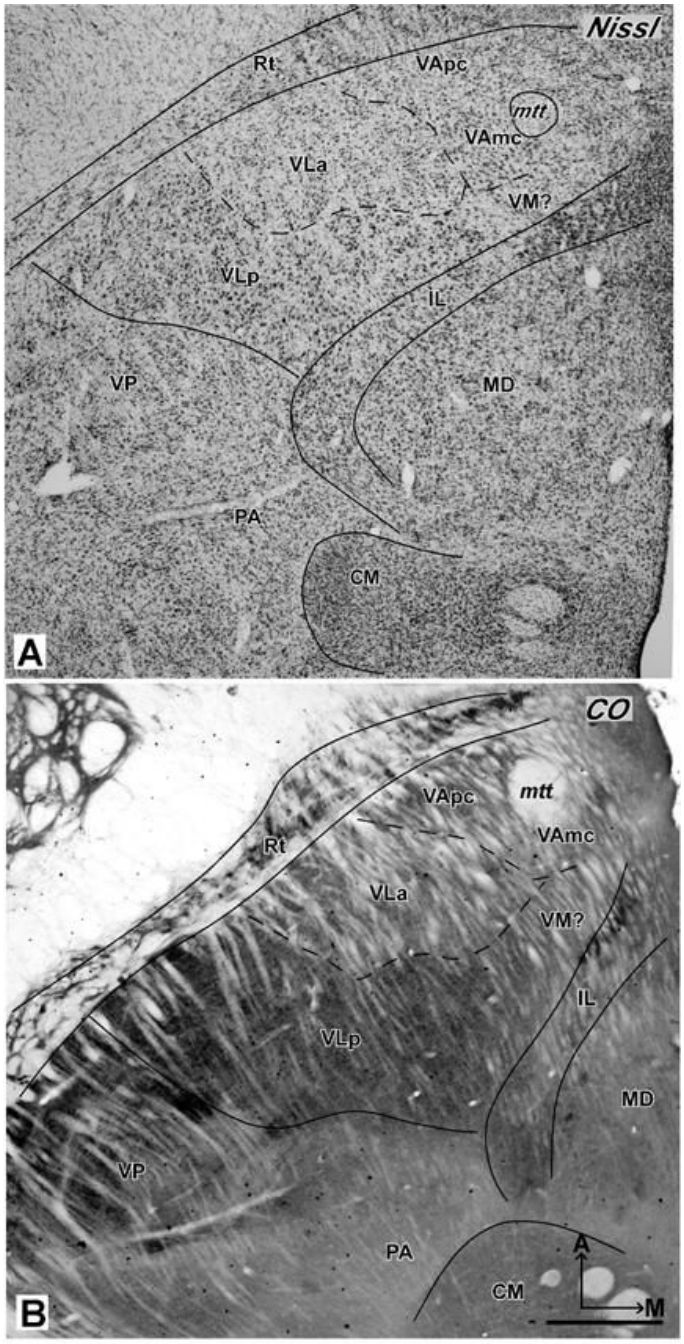

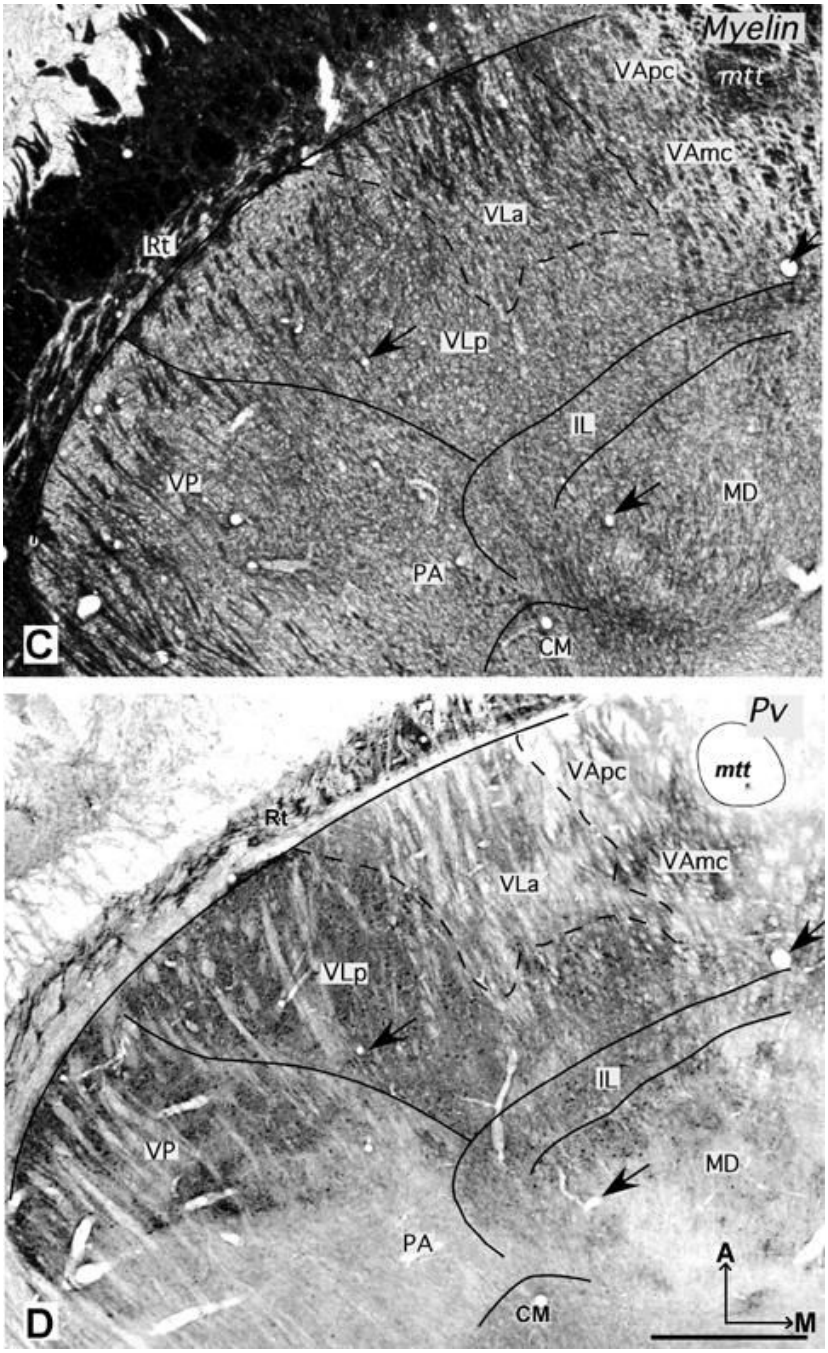

Fig 5.

Photomicrographs of horizontal sections processed for Nissl substance (**A**, case 03-19), CO (**B**, case 03-74), myelin or parvalbumin (**C** and **D**, case 03-19). VLp is darkly-stained in CO and Pv preparations, and VLa is dark in the myelin preparation. Arrows in **C** and **D** mark corresponding blood vessels. Other conventions as in figure 2. Scale bar = 1 mm.

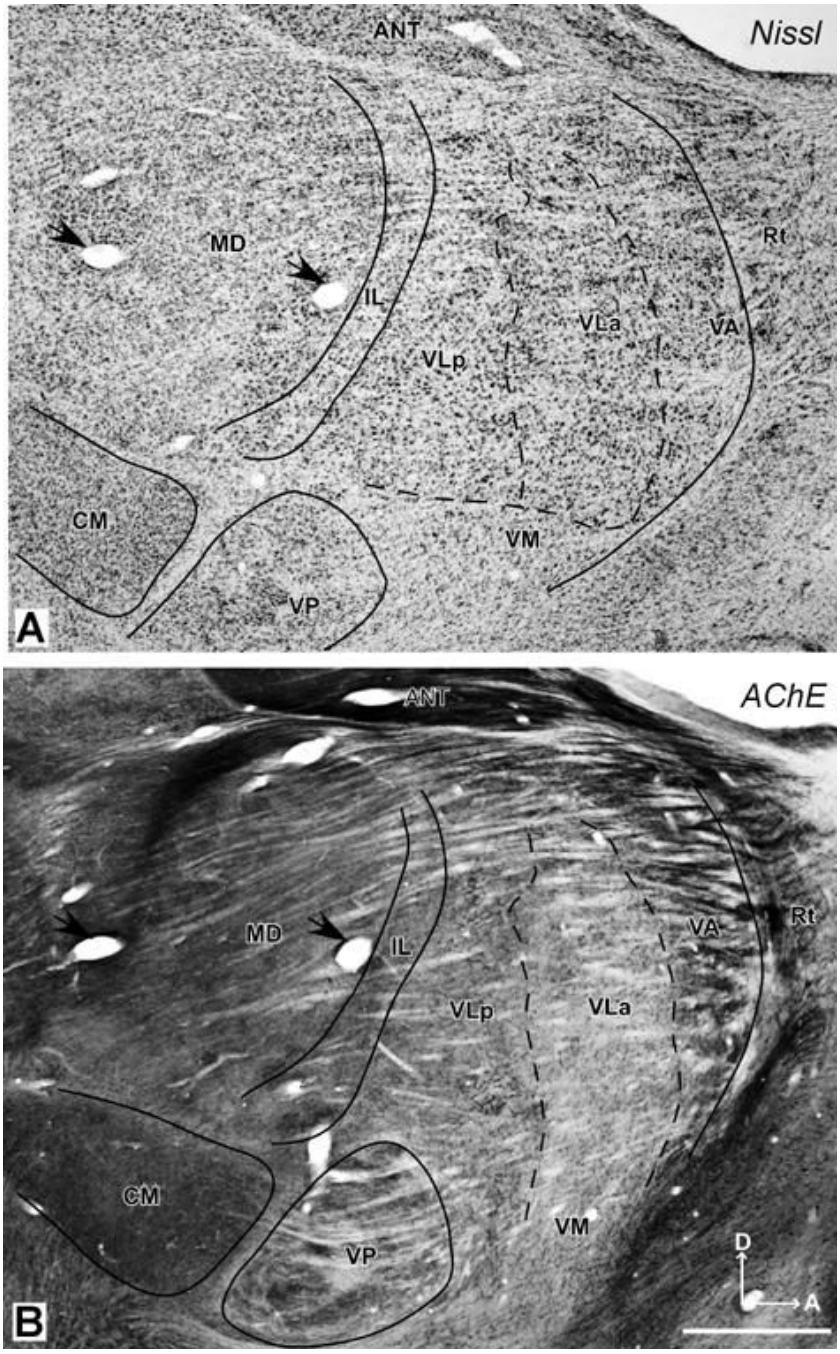

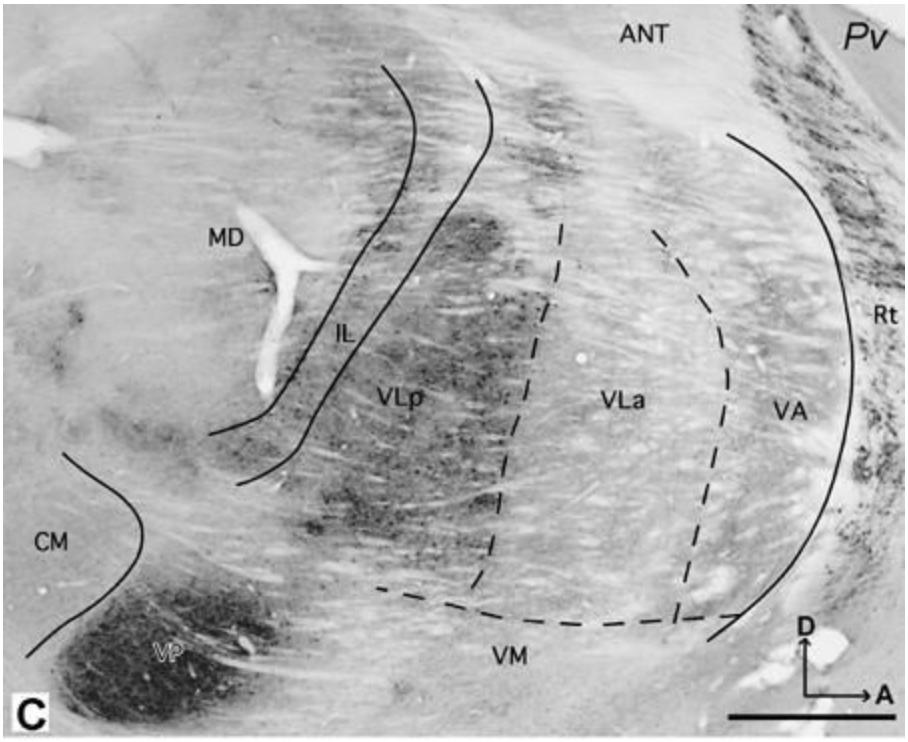

Fig 6.

Photomicrographs of sagittal sections from galago 03-56 stained for Nissl substance (**A**) or AChE (**B**), and from galago 03-43 stained for parvalbumin (**C**). In the Nissl preparation, subdivisions of motor thalamus are not obvious. In the AChE and Pv preparations, the main subdivisions of the motor thalamus, VLp, VLa, and VApc can be demarcated clearly. D = dorsal. Other conventions as in figure 2. Scale bar = 1 mm.

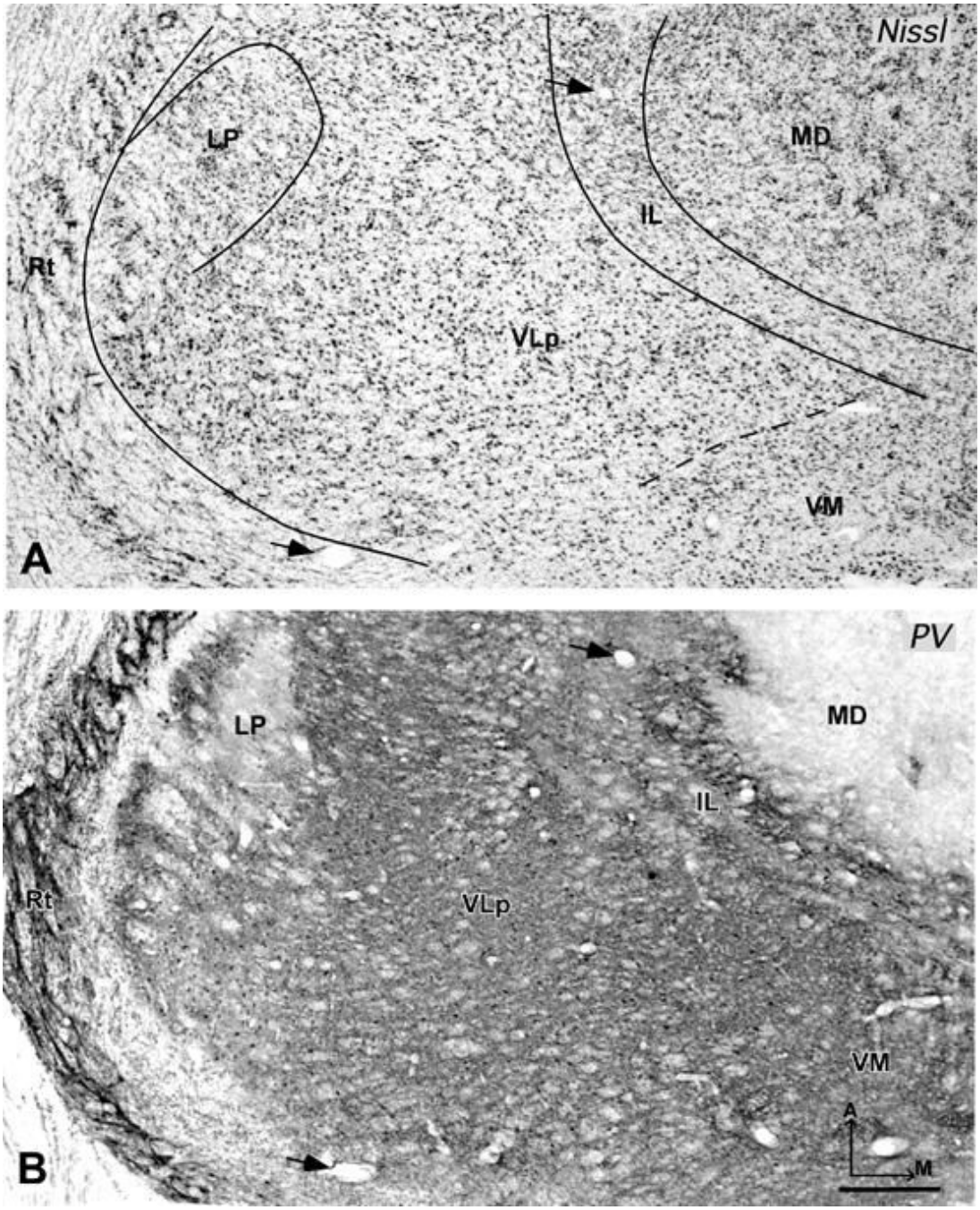

Fig 7.

Photomicrographs of coronal sections stained for Nissl (galago 03-56) and Pv (galago 03-12). In the Nissl preparation (**A**), the VLp has bigger and darker cells than the ventrally adjacent VM, and especially the dorsally adjacent LP. In the Pv preparation (**B**), VLp is distinguished as darkly-stained structure, and LP is much lighter. Arrows mark corresponding blood vessels. Other conventions as in figure 2. Scale bar = 0.5 mm.

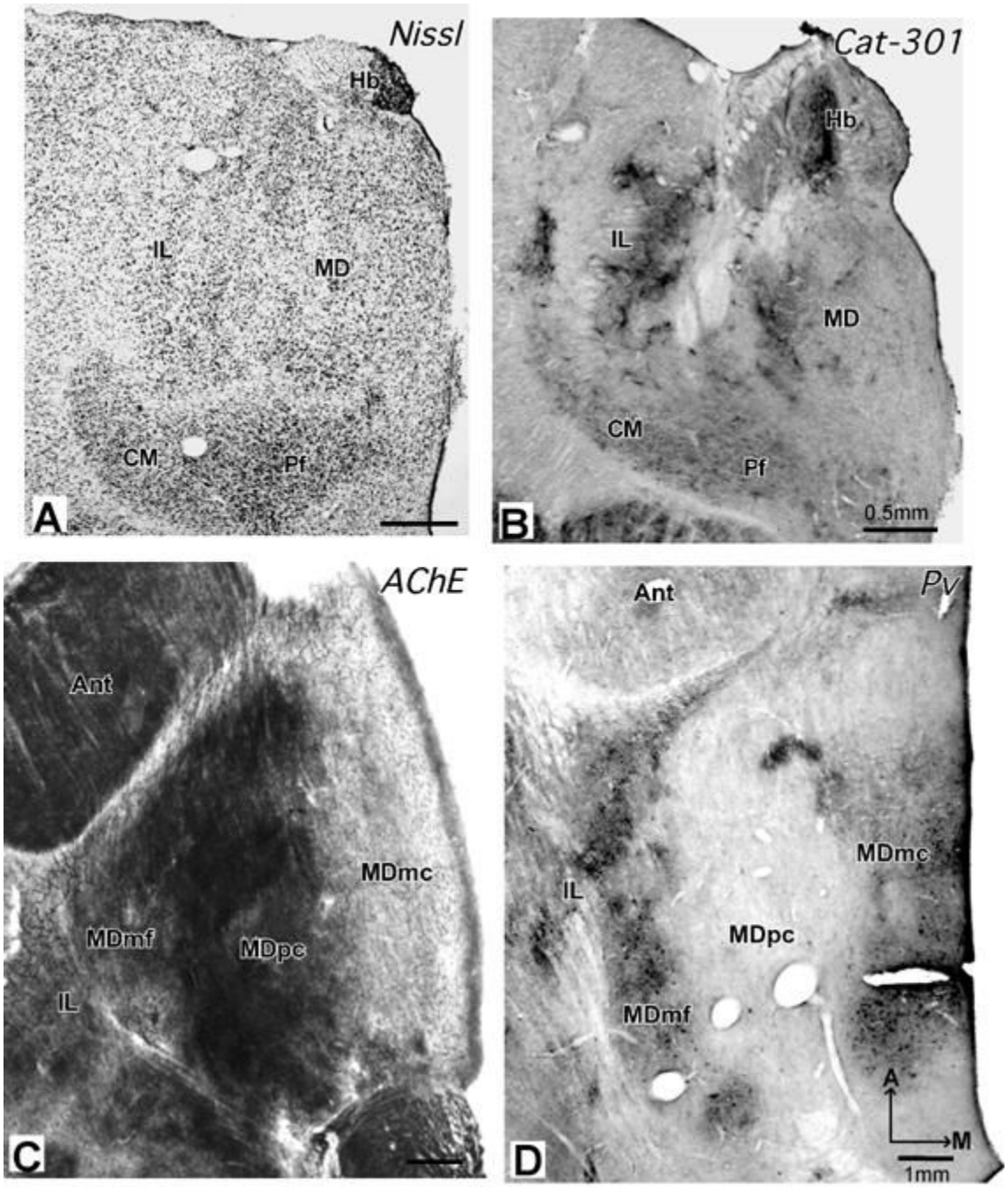

Fig 8.

Photomicrographs of coronal (**A** and **B**) and horizontal (**C** and **D**) sections through MD and CM/Pf nuclei. (**A**) In the Nissl preparation (galago 03-56), CM/Pf is more darkly-stained and more densely packed with cells than adjacent structures. (**B**) In the Cat 301 preparation (galago 01-98), CM is uniformly and moderately stained (**C**). In the AChE preparation (galago 03-74), MDpc is the most darkly stained MD subdivision, whereas MDmf is stained moderately and MDmc is quite pale.(**D**) In the Pv preparation (galago 03-19), MDmf is darkly-stained, MDmc is moderately-stained and MDpc is pale. Other conventions as in figure 2. Scale bar = 0.5 mm (A+B) and 1 mm (C+D).

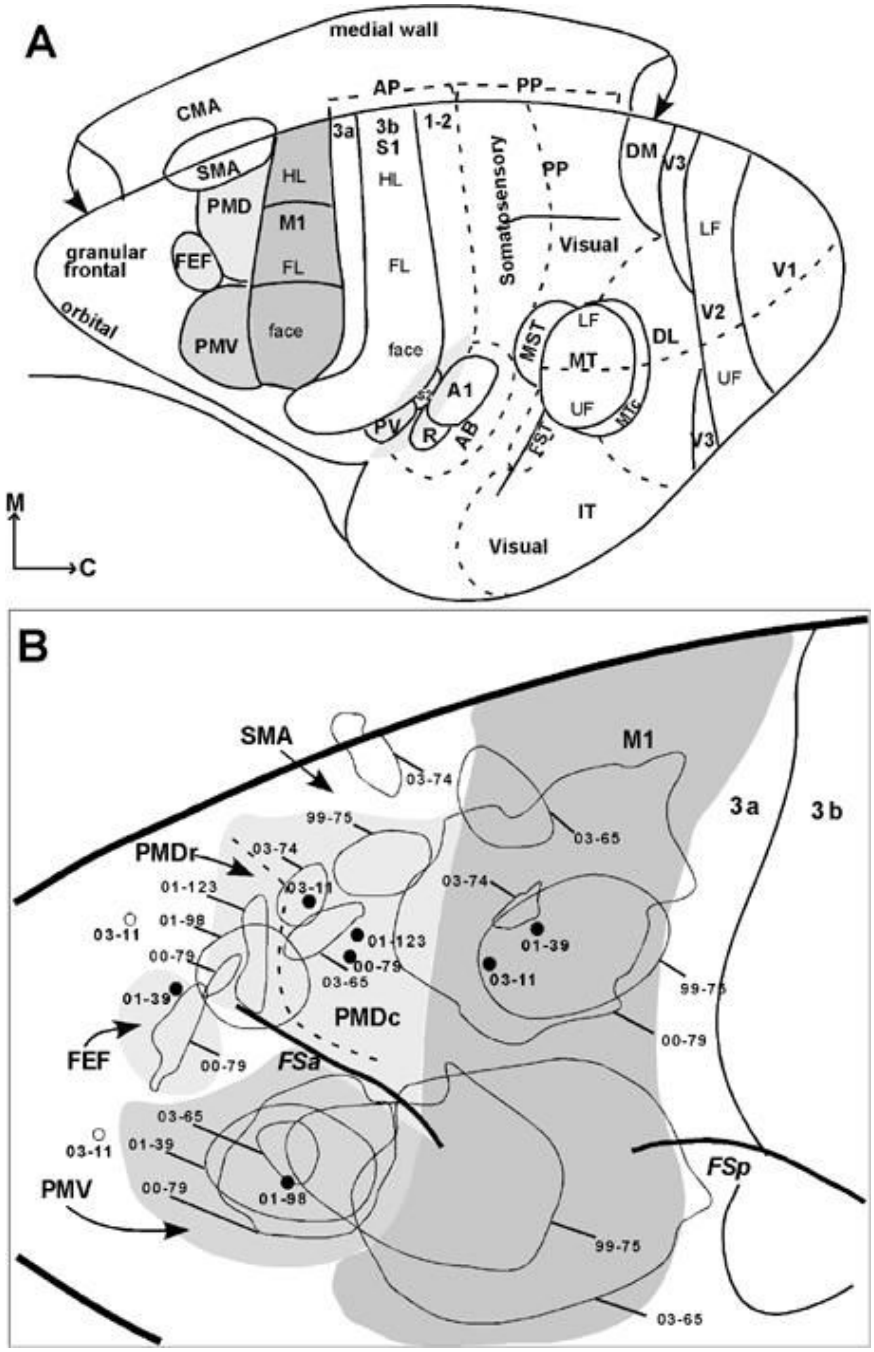

Fig 9.

Subdivisions of cortex and injection sites in galagos. (**A**) The primary motor area (M1) is dark gray. The ventral premotor area (PMV) is gray, and the dorsal premotor area (PMD) and the frontal eye field (FEF) are light gray. M1 represents the hindlimb/trunk (HL), forelimb (FL) and face from medial to lateral. PMV in galagos includes mostly orofacial movements and a few upper trunk movements, and the caudal PMD includes hindlimb/trunk and forelimb movements. Motor areas are shown relative to somatosensory, auditory, and visual areas described elsewhere (Kaas, 2004). Somatosensory areas include the primary area, S1 or area 3b, and areas 3a and 1-2 of anterior parietal (AP) cortex. Posterior parietal cortex (PP) has an anterior sector with somatosensory inputs and a posterior sector with visual inputs. The parietal

ventral area (PV) and the second area (S2) are secondary somatosensory fields. Auditory areas include the primary area (A1), the rostral area (R), and the auditory belt (AB). Visual areas include the first, second, and third areas (V1, V2, and V3), the dorsolateral area (DL), the dorsomedial area (DM), the middle temporal area (MT), the medial superior temporal area (MST), the MT crescent (MTc), the fundal superior temporal area (FST), and inferior temporal (IT) cortex. Upper (UF) and lower (LF) field representations are indicated in V2 and MT. (**B**) Summary of the locations of tracer injections in the motor fields and the prefrontal cortex in eight cases. The injection cores are marked with thin outlines, whereas open circles (case 03-11) indicate injection sites. Cases marked with solid dots are described but not illustarted. The injection cores for these cases are shown on individual brain figures in Fang et al. (2005).

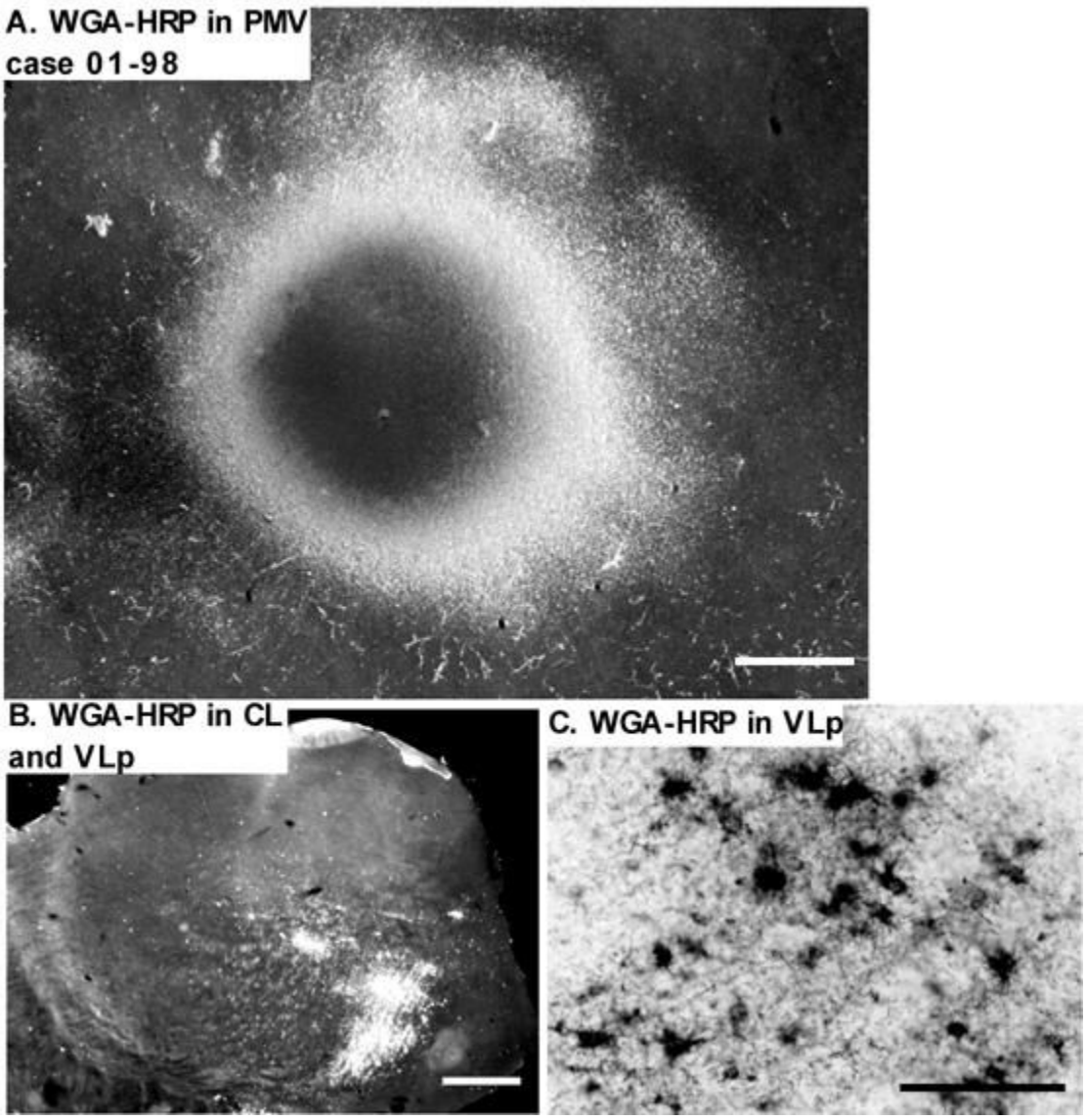

Fig 10.

Photomicrographs of the WGA-HRP injection in case 01-98. (**A**) The injection site was in the orofacial representation of PMV. The dense core in the center is surrounded by the outer ring of dense transport. Labeled perikarya and fibers are visible just outside this ring. Scale bar = 1mm. (**B**) Dense retrograde and anterograde labeling in the thalamus in a coronal thalamic section following the injection in the cortex. Dense labeling appears in VLp and CL. Top = dorsal; Left = lateral.; Scale bar = 1mm. (**C**) A higher magnification showing the retrogradely labeled cells and fibers in VLp. Perikarya are filled with WGA-HRP and the proximal dendrites are visible in most of the cells. Scale bar = 100μm.

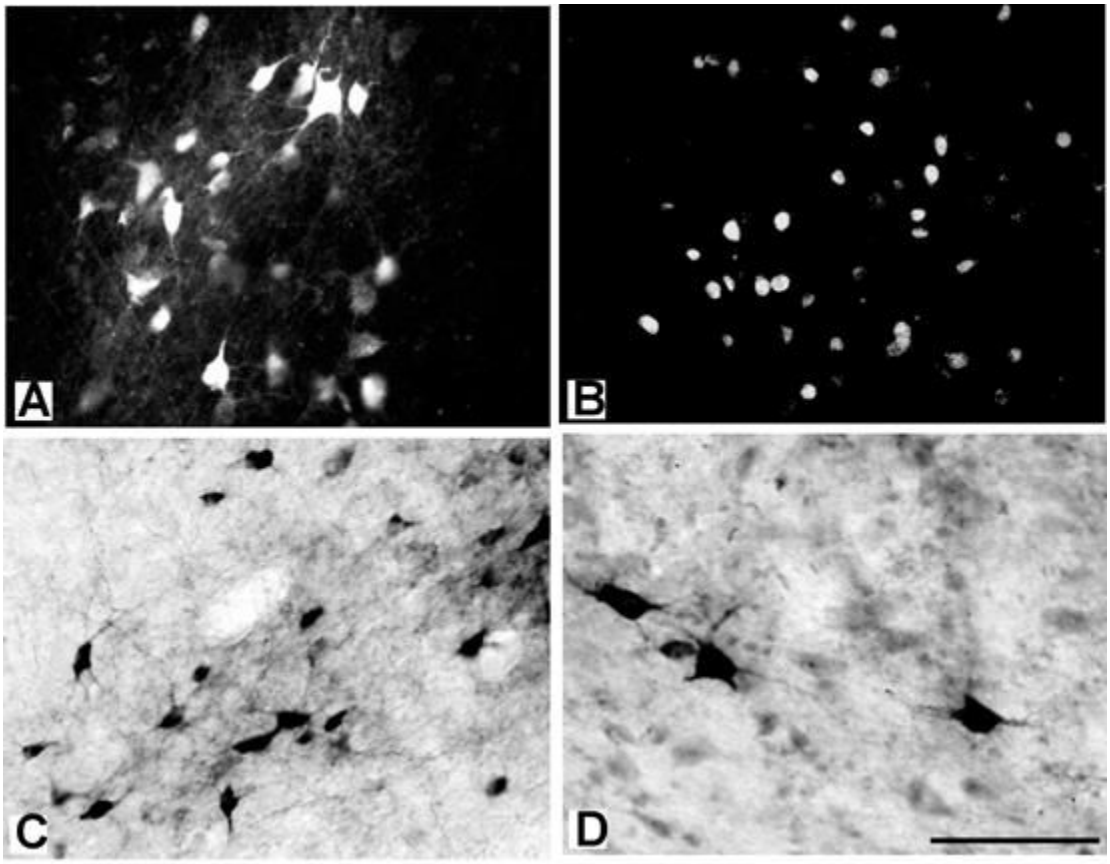

Fig 11.

Photomicrographs of the labeled cells in the thalamus after the injections in the motor cortex. (**A**) The cell bodies and dendrites of the central lateral (CL) thalamic cells labeled by FR placed into PMD in case 03-65. (**B**) Nuclei of neurons in VLa labeled by DY placed into M1 orofacial area in case 03-65. (**C**) The cell bodies and dendrites of neurons in VLp labeled by a BDA injection in PMV in case 03-65. (**D**) The cell bodies and proximal dendrites of neurons in VLp labeled by a CTB injection in PMD in case 03-74. Scale bar = 100 μm.

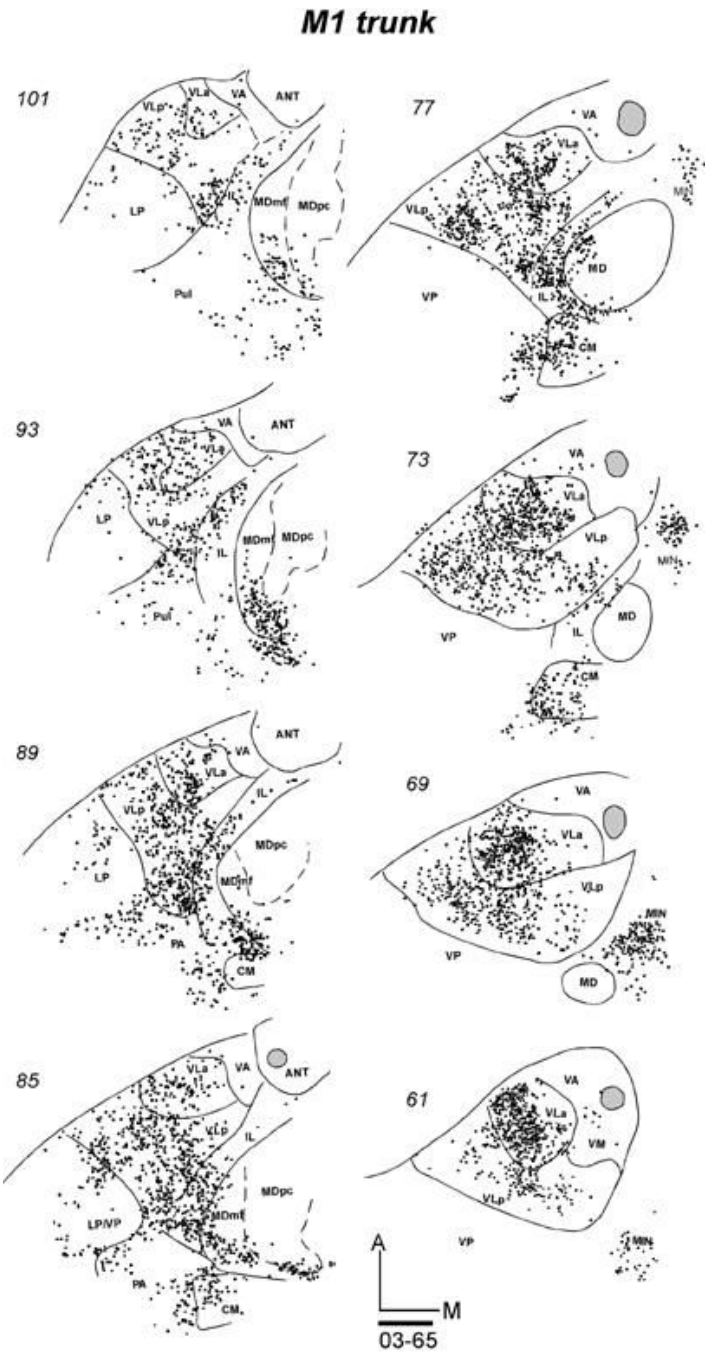

Fig 12.

The distribution of CTB labeled cells in a series of horizontal sections from dorsal (101) to ventral (61) of the thalamus in case 03-65 after CTB was injected into the trunk representation of M1. The injection site in the cortex partly involved SMA trunk and M1 forelimb and hindlimb representations. In this case, the injection possibly involved some white matter. Each dot represents a single labeled cell. Scale bar = 1 mm.

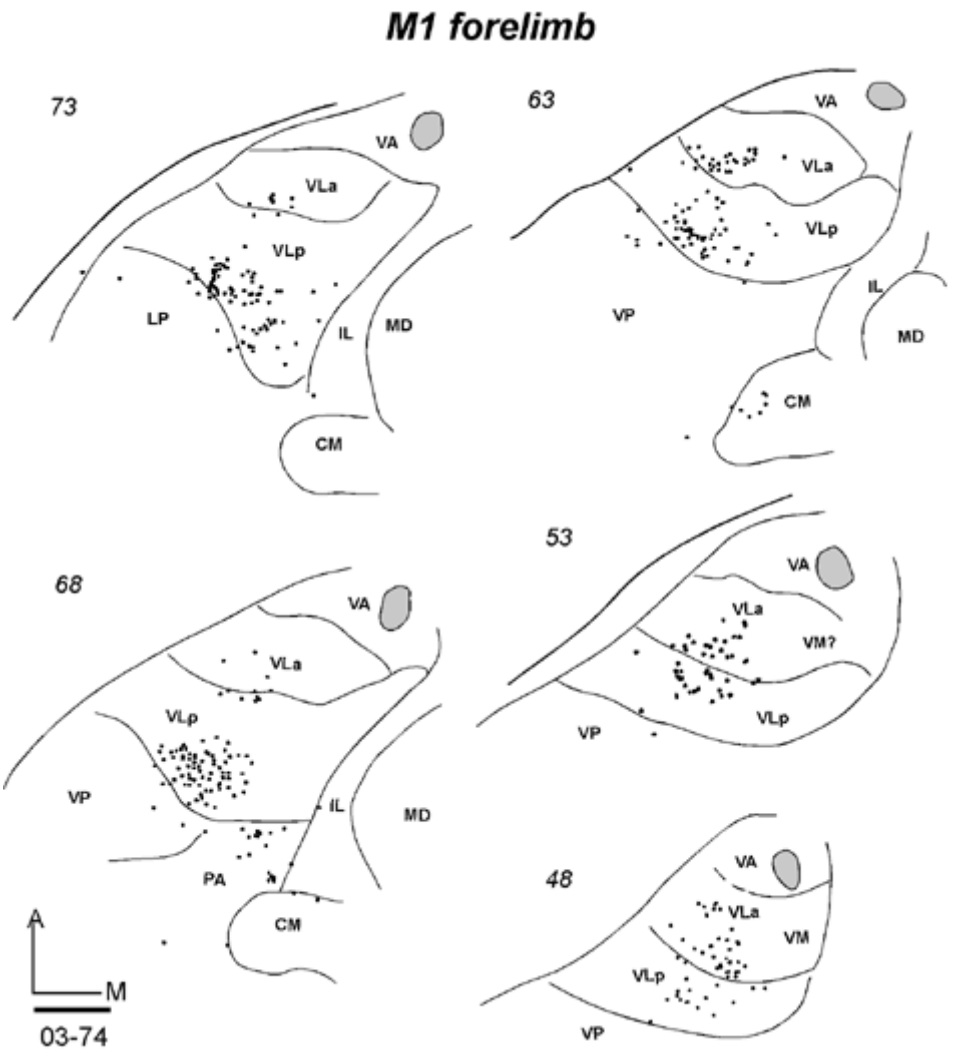

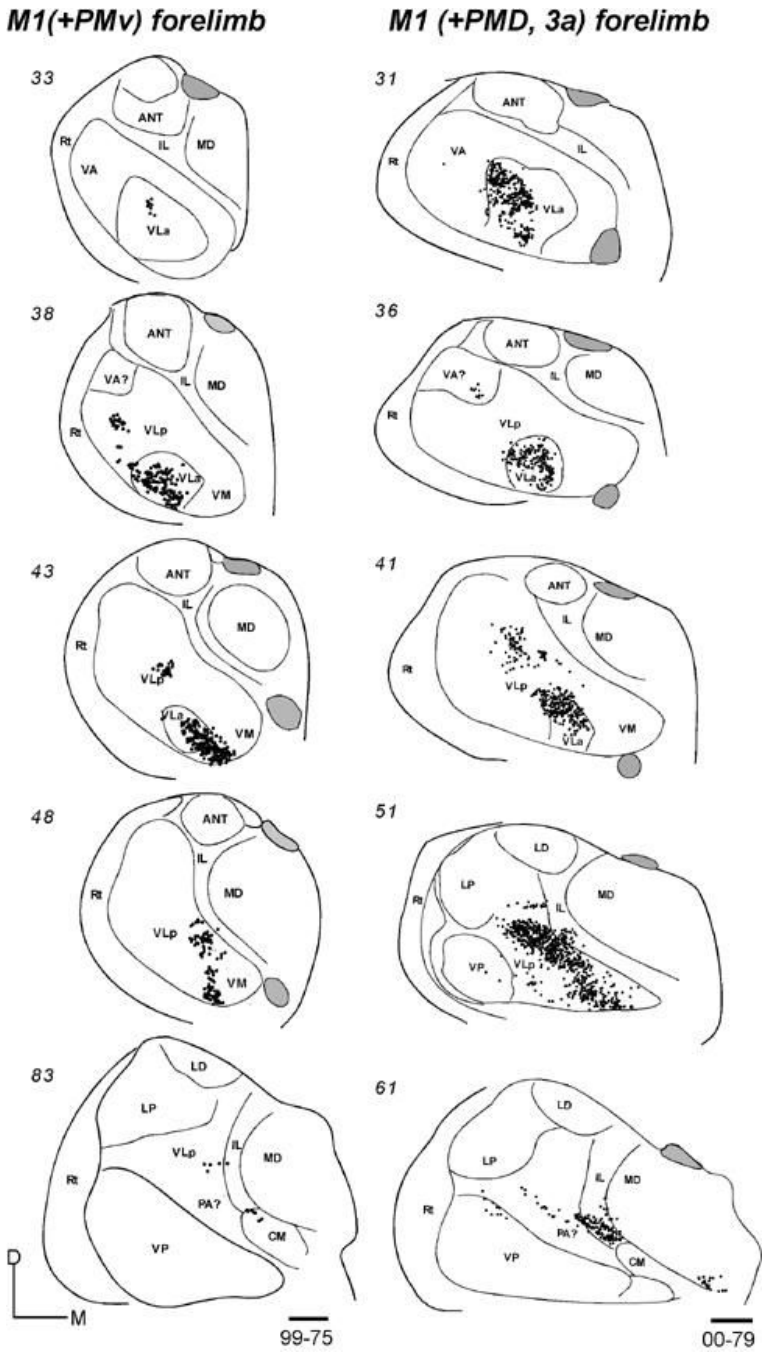

Fig 13.

A series of thalamic sections of three galagos with tracer injections in the M1 forelimb representation. (**13-1**) Labeled neurons in horizontal sections from dorsal (73) to ventral (48) following an injection of FE confined to the M1 forelimb area in case 03-74. (**13-2 left**) Labeled neurons in coronal sections from anterior (33) to posterior (83) after a WGA-HRP injection was restricted to the forelimb representation of M1 in case 99-75. (**13-2 right**) Labeled neurons in coronal sections from anterior (31) to posterior (61) in case 00-79 after a DY injection in the M1 forelimb area that also involved parts of PMD and area 3a. Scale bar = 1 mm.

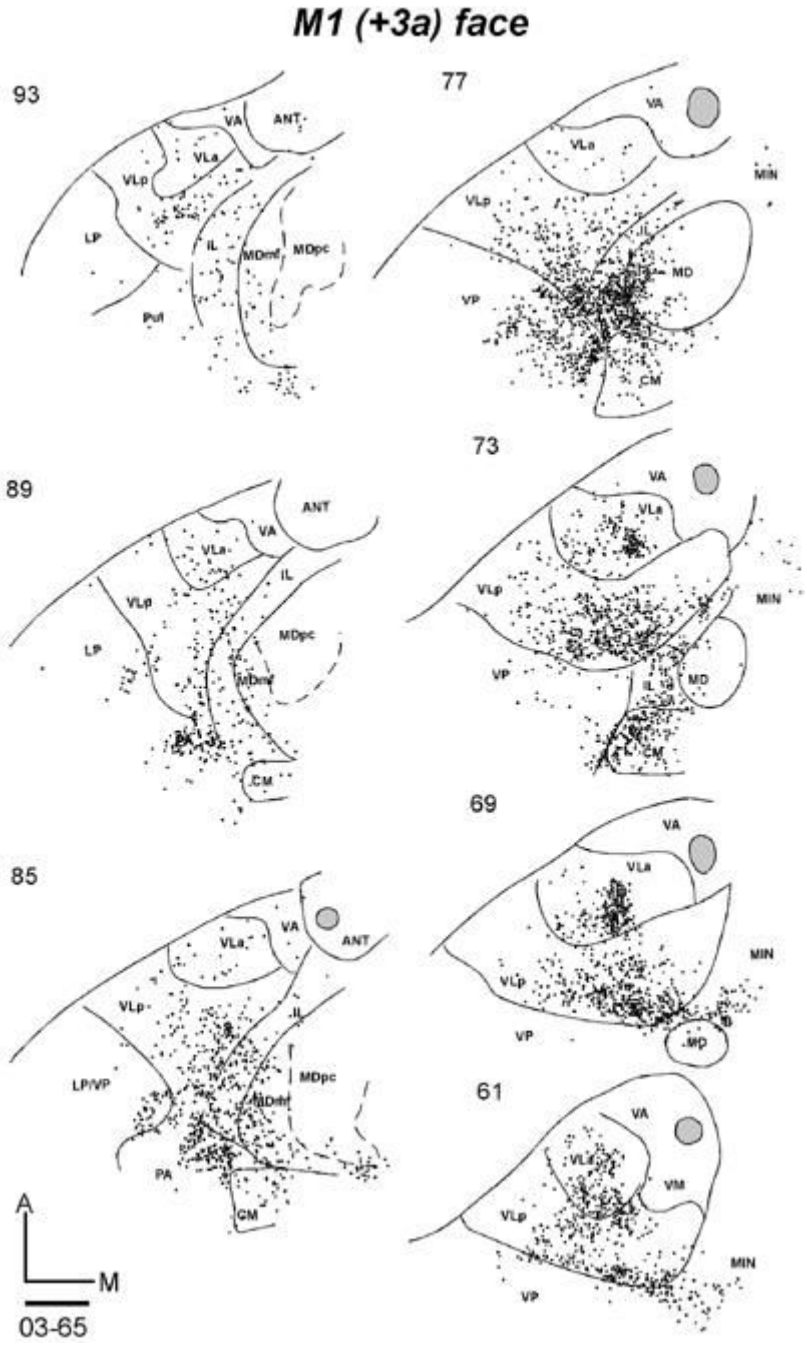

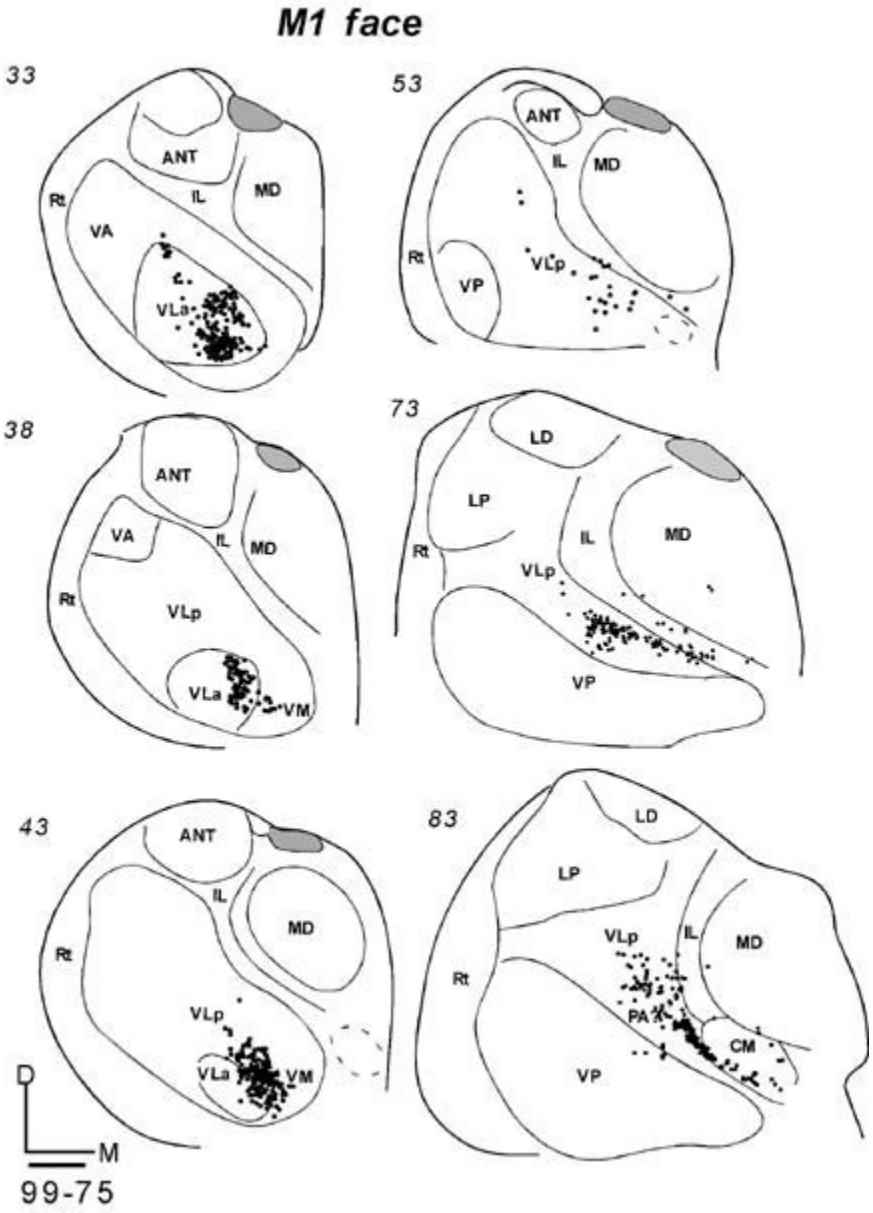

Fig 14.

Distributions of labeled cells in two cases following the injections of fluorescent tracers in the M1 orofacial representation. Both injections had large uptake zones that covered PMV. (**14-1**) The DY injection in case 03-65 also involved area 3a. Labeled cells (dots) are shown in horizontal sections from dorsal (93) to ventral (61). (**14-2**) Labeled cells in coronal sections from anterior (33) to posterior (83) in case 99-75 with a FB injection. Scale bar = 1 mm.

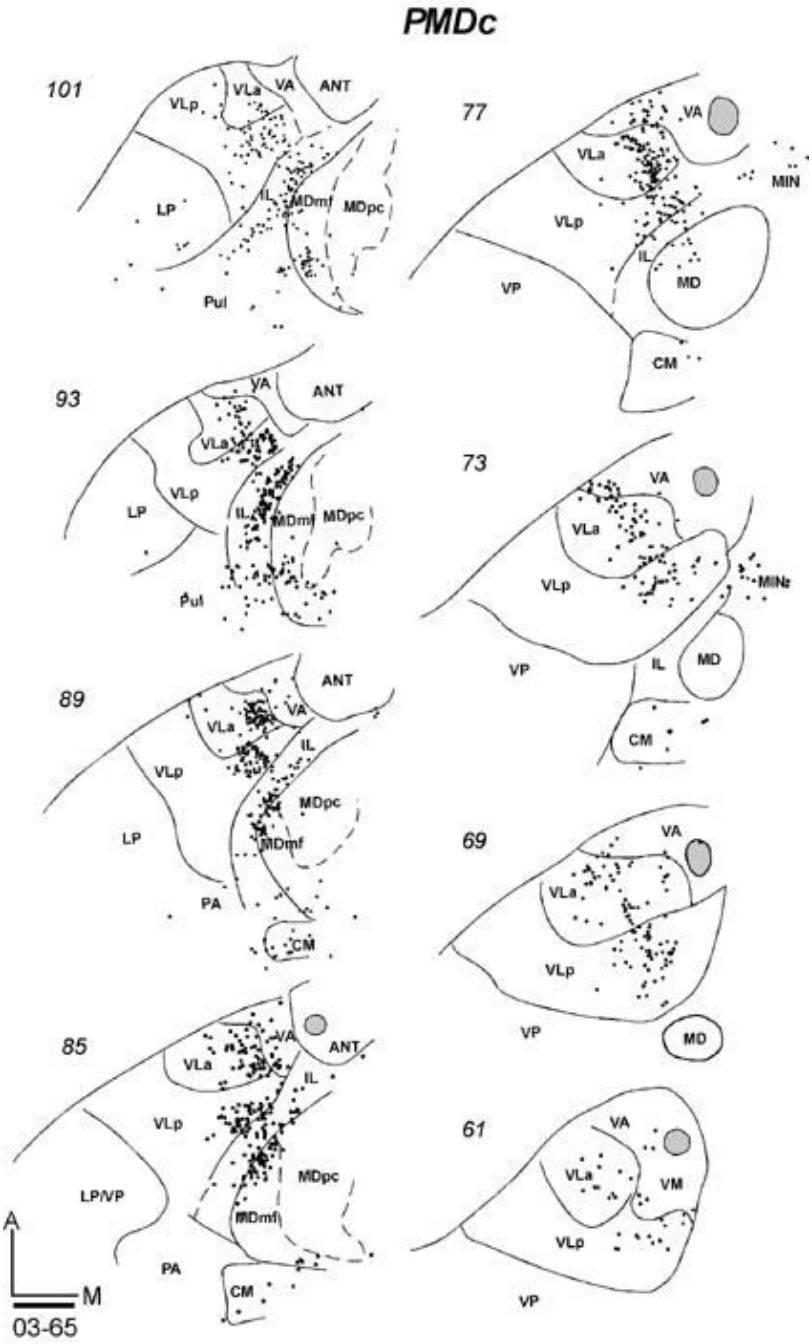

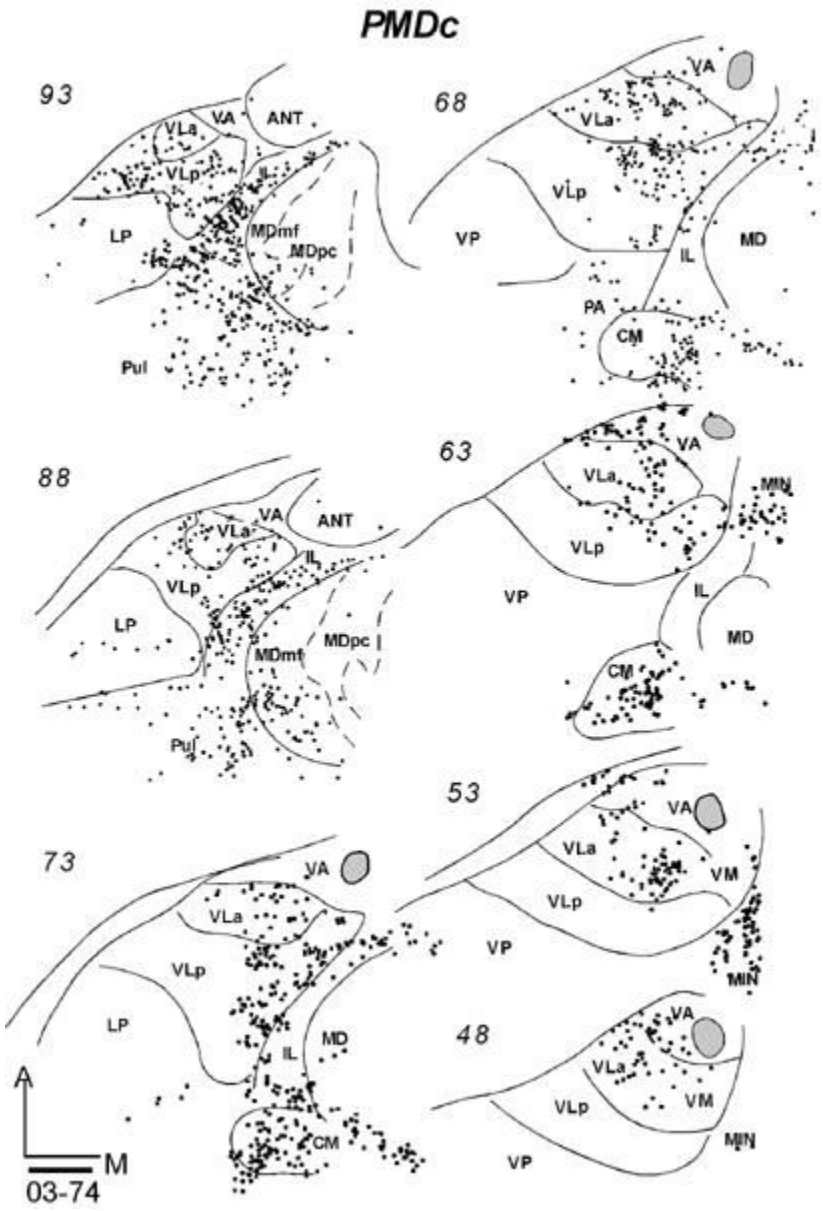

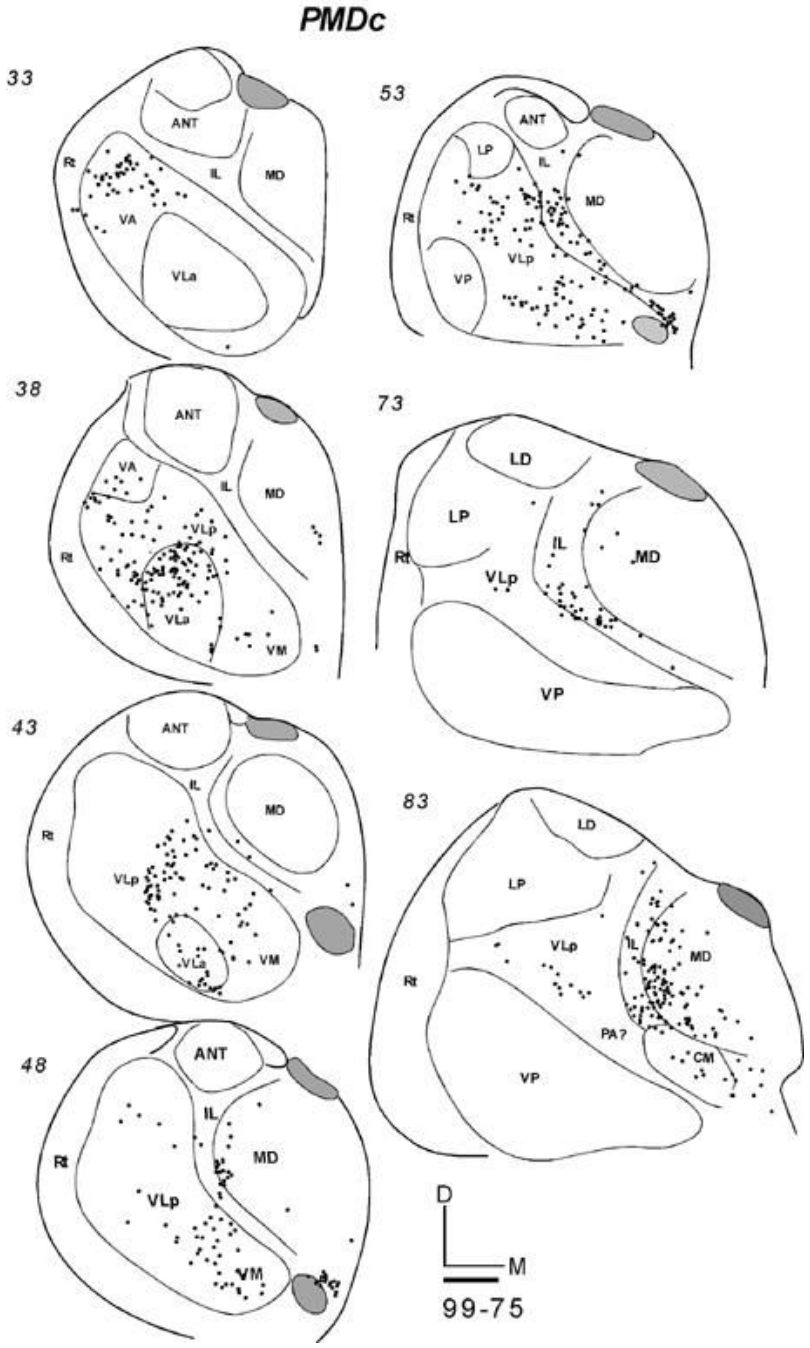

Fig 15.

Distributions of labeled cells in the thalamus following tracer injections in PMDc of three galagos. All injections were confined to PMD. (**15-1**) Labeled cells in horizontal thalamic sections from dorsal (101) to ventral (61) in case 03-65 with a FR injection. (**15-2**) Labeled cells in horizontal thalamic sections from dorsal (93) to ventral (48) in case 03-74 with a CTB injection. (**15-3**) Labeled cells in coronal sections from rostal (33) to caudal (83) in case 99-75 with a FR injection. Scale bar = 1mm.

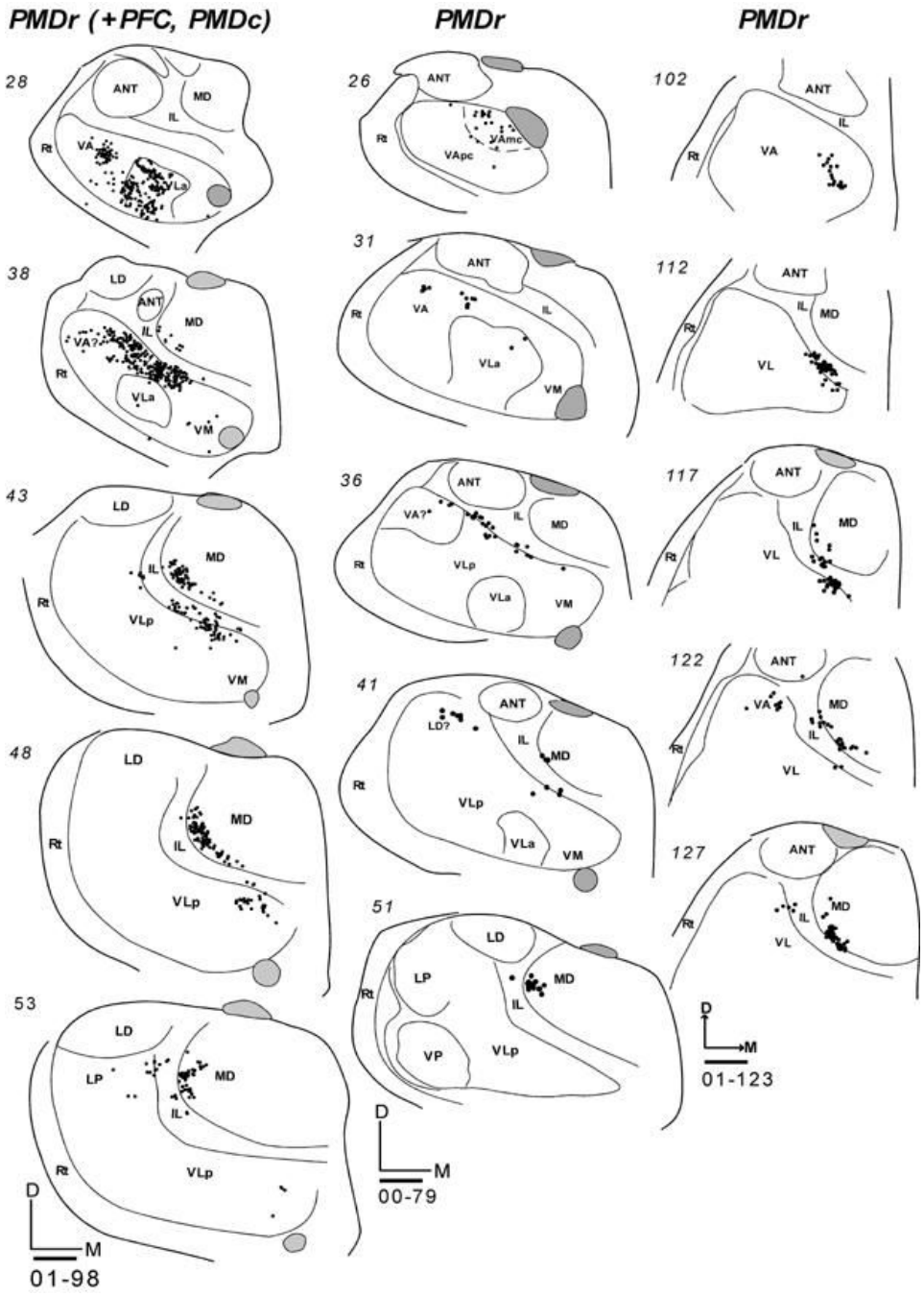

Fig 16.

Labeled cells in coronal thalamic sections from rostral (top) to caudal (bottom) following tracer injections in PMDr of three galagos. All injections were confined to PMD. (**Left**) Labeled cells in coronal thalamic sections in case 01-98 with a DY injection. This injection was large and included parts of caudal PMD and prefrontal cortex. (**Middle**) Labeled cells in coronal sections in case 00-79 with a FE injection. (**Right**) Labeled cells in coronal sections in case 01-123 with a FE injection. Scale bar = 1mm.

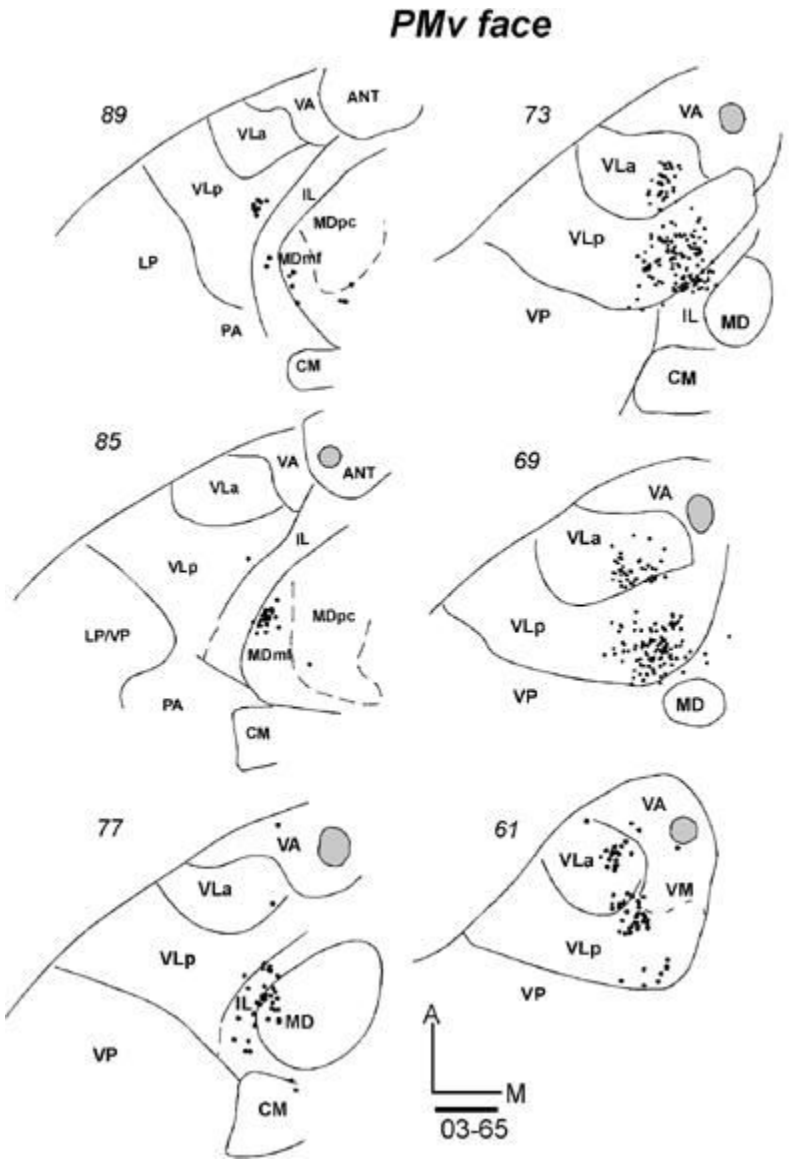

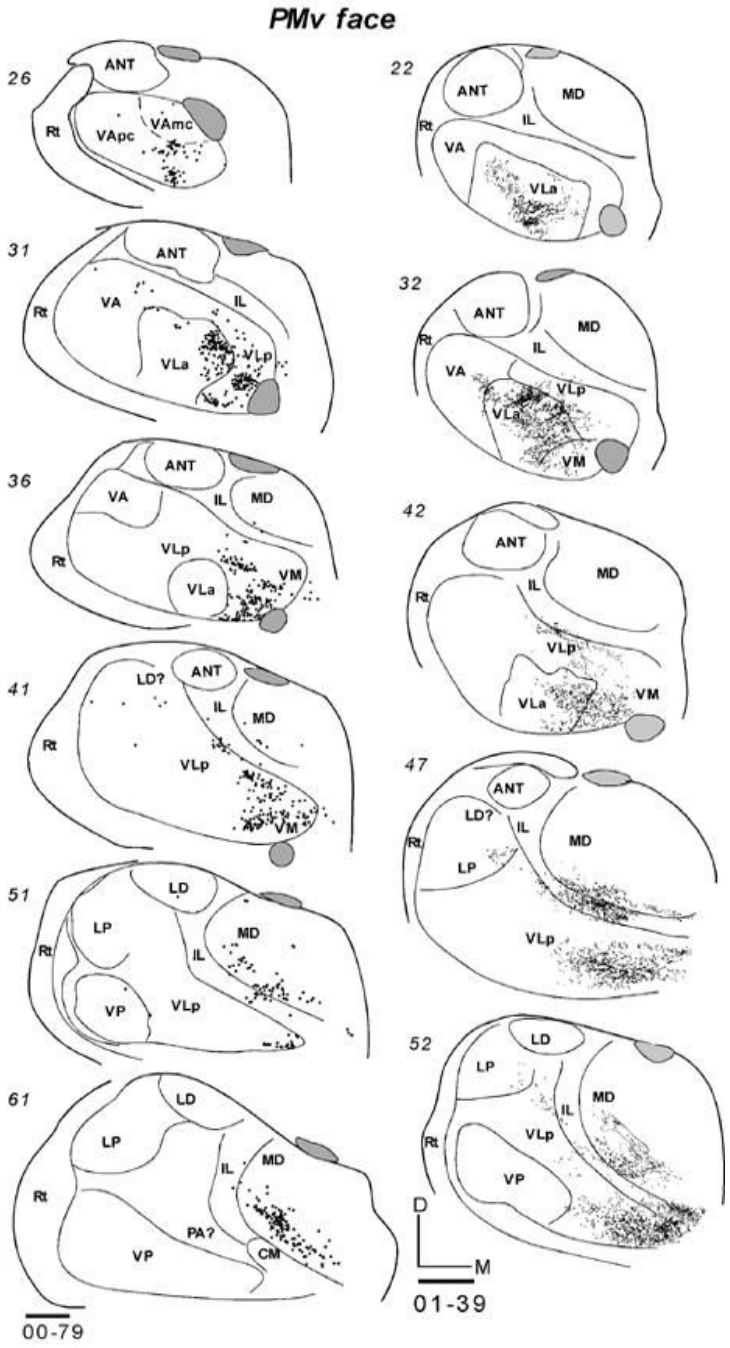

Fig 17.

Labeled cells in the thalamic sections following injections in PMV orofacial representation in three galagos. (**17-1**) Labeled cells in horizontal sections from dorsal (89) to ventral (61) after a BDA injection in case 03-65. (**17-2 left**) Labeled cells in coronal sections from rostral (26) to caudal (61) in case 00-79 with a FB injection. (**17-2 right**) Labeled neurons from rostral (22) to caudal (52) in case 01-39 with a WGA-HRP injection. Scale bar = 1 mm.

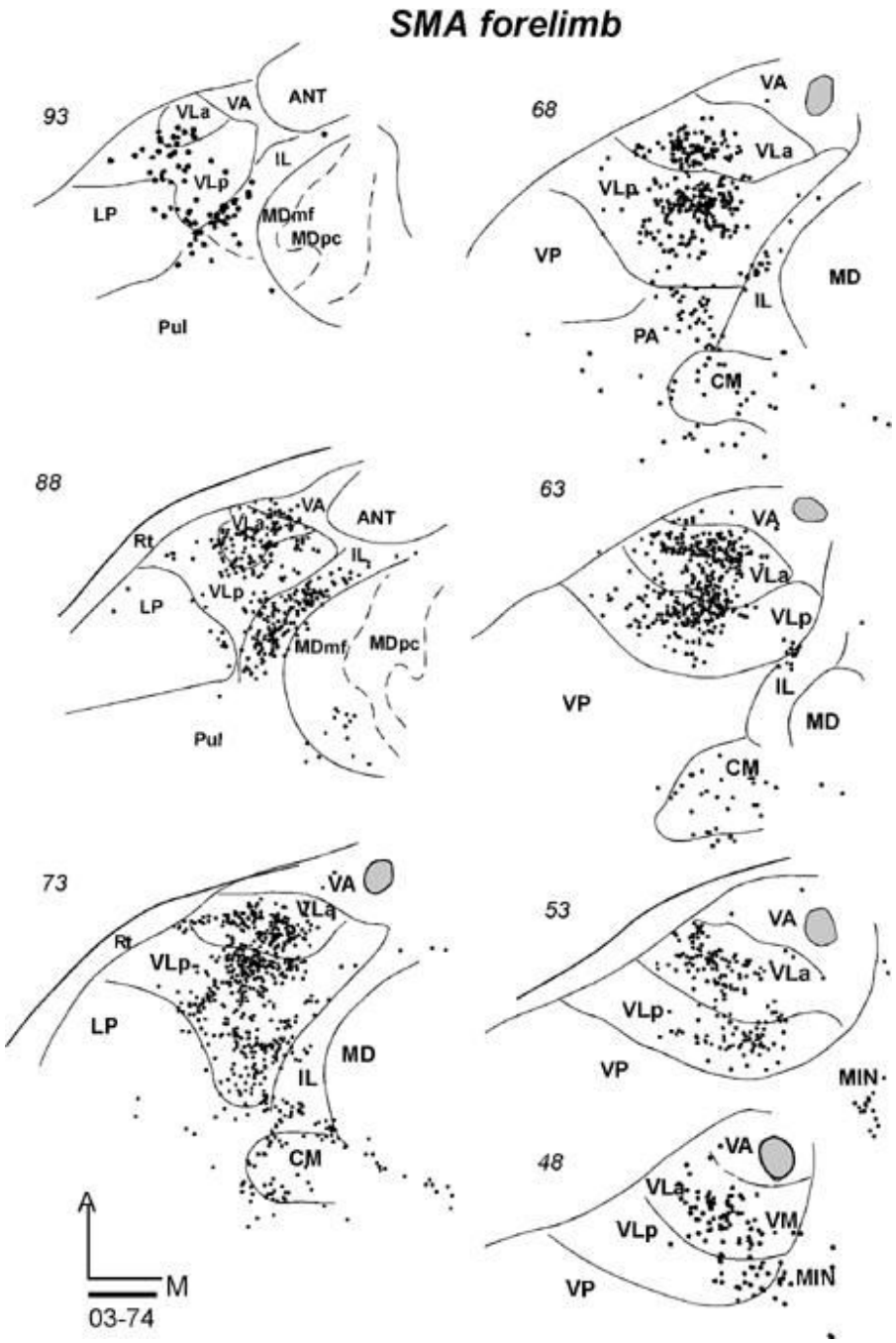

Fig 18.

Labeled neurons in a series of horizontal sections from dorsal (93) to ventral (48) of the thalamus of case 03-74 with a FR injection confined to the forelimb representation of SMA. Scale bar = 1mm.

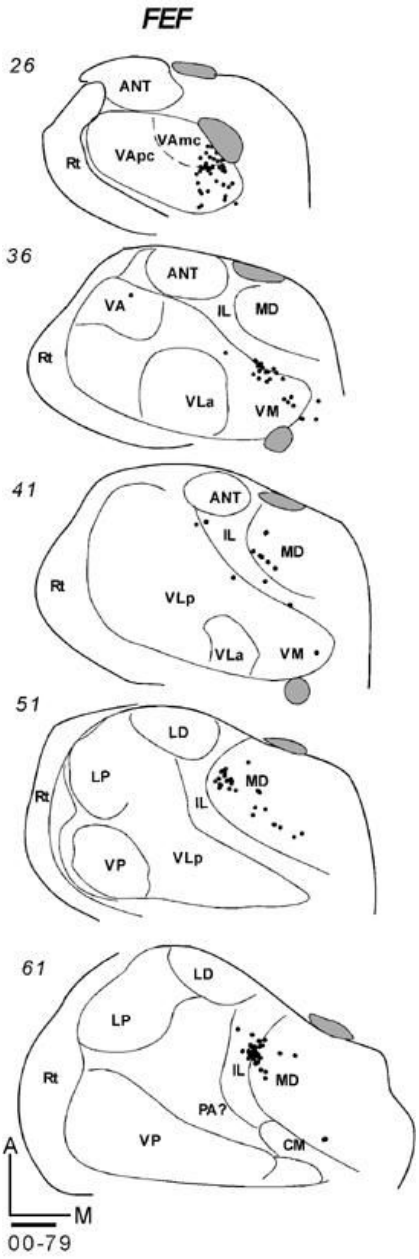

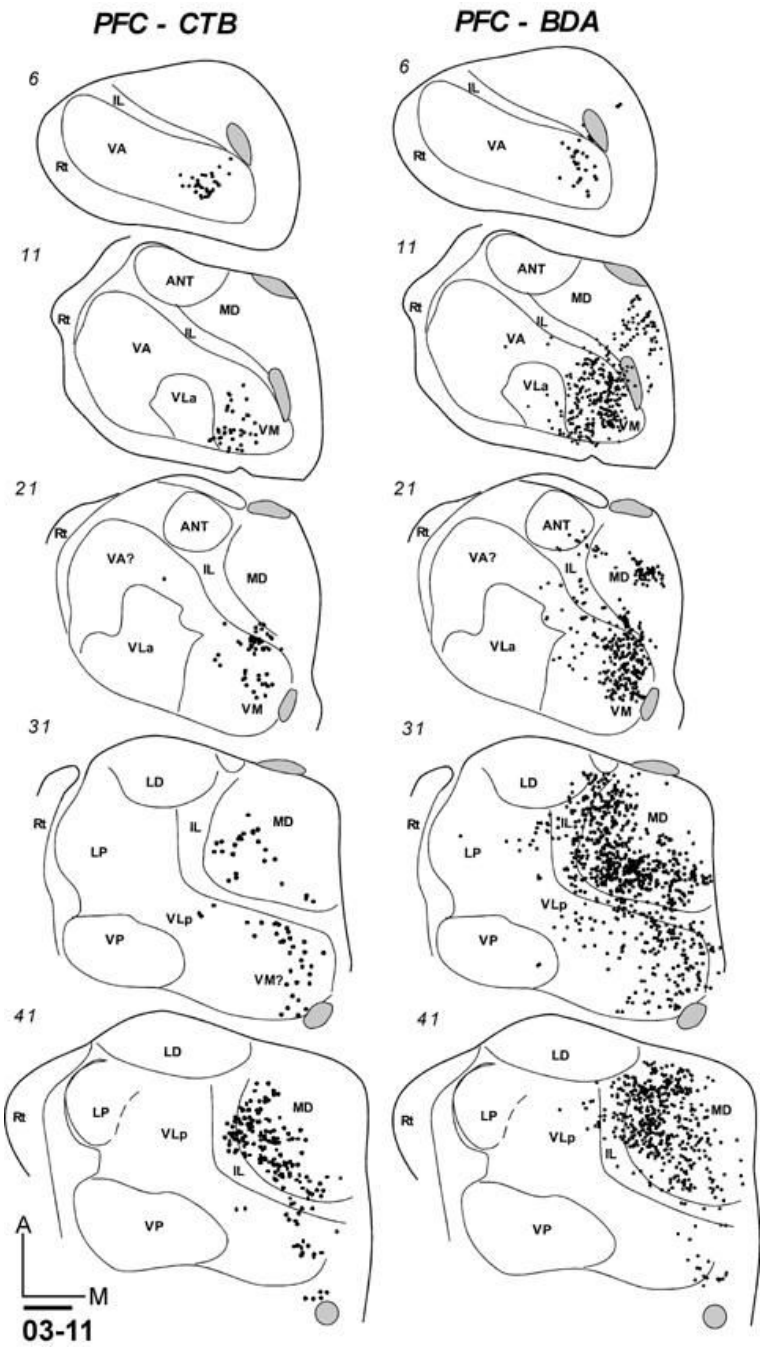

Fig 19.

Labeled neurons in series of coronal sections from anterior (top) to posterior (bottom). (**19-1**) Galago 00-79 had a FR injection confined to FEF. (**19-2 left**) Galago 03-11 had a CTB injection in prefrontal cortex just anterior to PMD. (**19-2 right**) Labeled neurons in galago 03-11 after a BDA injection in prefrontal cortex just anterior to PMV. Scale bar = 1mm.

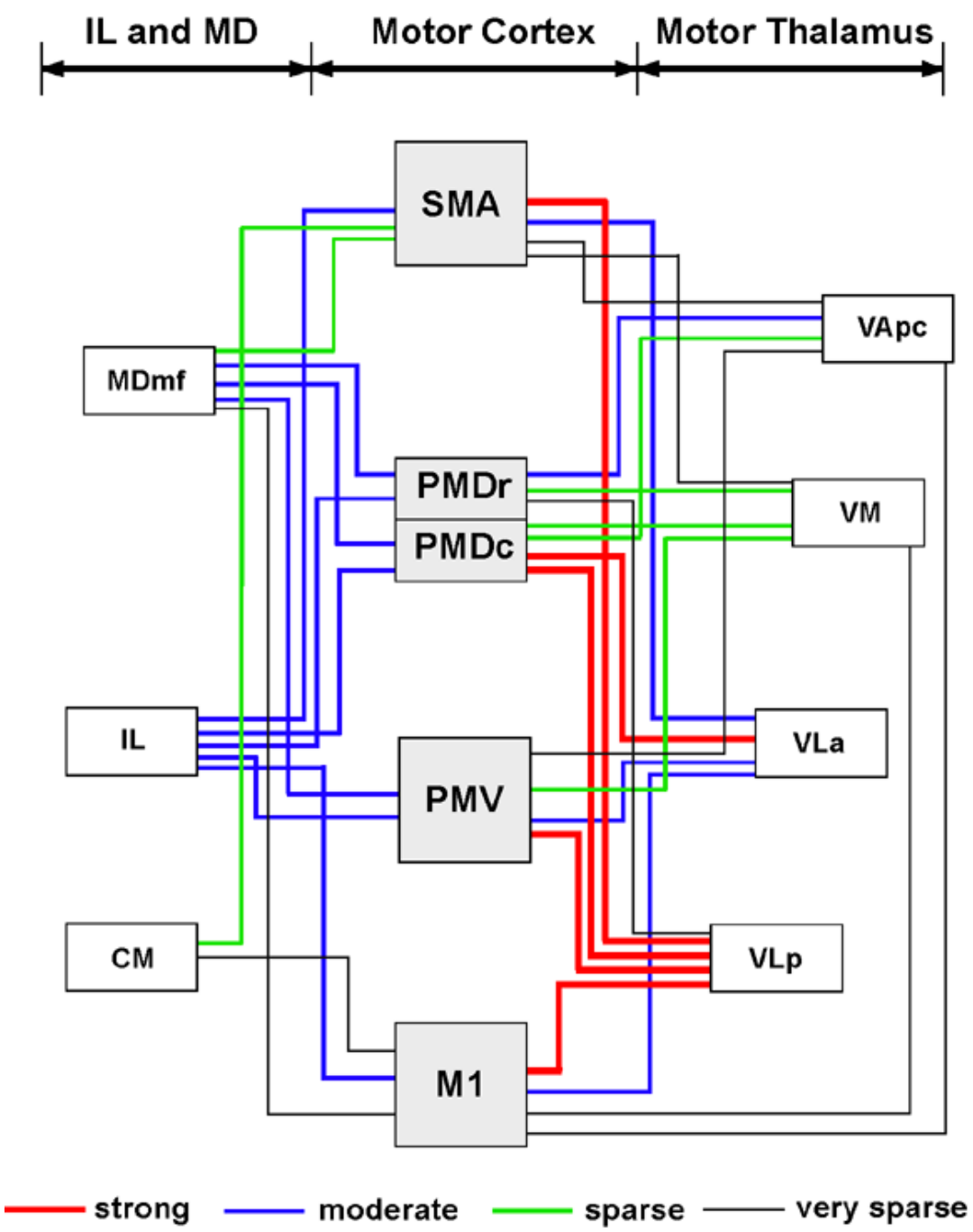

Fig 20.

A summary of projections from the motor thalamus, IL and MD to four motor fields of galagos. The VL complex of the motor thalamus contributes the most inputs to the motor cortex, with VLp more densely connected to M1, PMV, SMA and PMDc, and VLa to PMDc. Of the other thalamic nuclei, intralaminar nuclei send moderate inputs to motor cortical regions, while MDmf projects mostly to PMD and PMV.

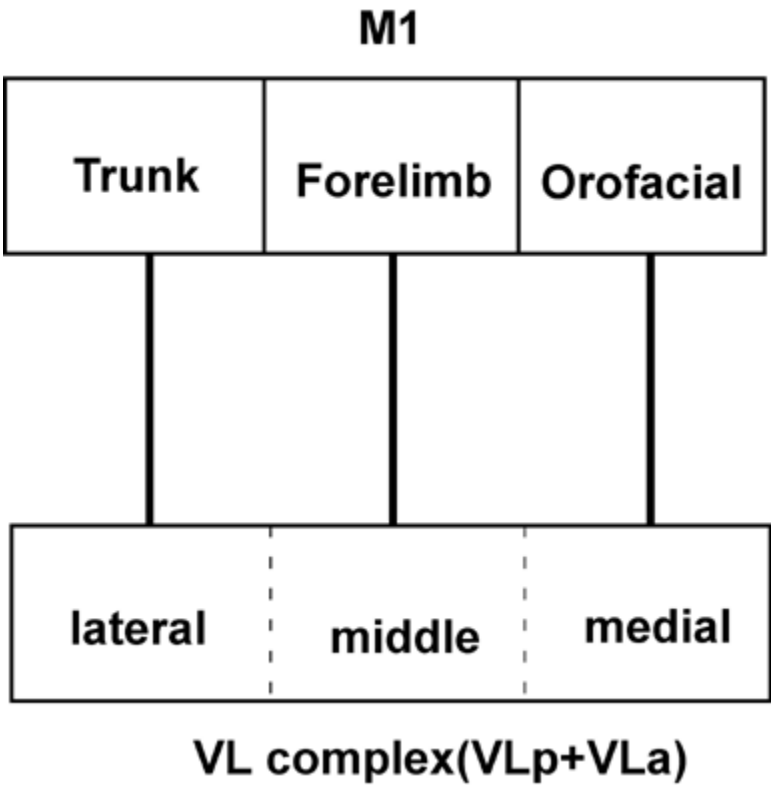

Fig 21.

The topographic organization of connections between ventral lateral complex of thalamic nuclei (VLa and VLp) and primary motor cortex (M1). Different motor cortical areas have dominant connections from different regions in the motor thalamus. The M1 trunk representation receives major projections from the lateral sector of VL, the forelimb representation receives connections mostly from the middle sector of VL, and the orofacial M1 representation receives major connections from the most medial VL.

Table 1

The cases, areas, and tracers injected.The thalami of cases 03-65 and 03-74 were cut horizontally, and the other cases were cut coronally. In case 03-11, additional two tracers were placed in the prefrontal cortex, CTB was in the cortex rostral to PMD and BDA was in the cortex rostral to PMV. Except for injections (DY in case 01-98, FE in case 00-79, and FE in case 01-123) in the rostral portion of PMD, injections were in the caudal portion of PMD.

Case Number		Tracers injected in the motor cortex						
		Tk/HL	M1 FL	OF	PMD FL	PMV OF	SMA FL	FEF
1	03-65	CTB		DY	FR	BDA		
2	03-74		FE		CTB		FR	
3	99-75		WGA-HRP	FB	FR			
4	00-79		DY		WGA-HRP,FE	FB		FR
5	01-39		DY			WGA-HRP		FB
6	01-98				DY	WGA-HRP		
7	01-123				WGA-HRP,FE			
8	03-11		FR		FE			

Table 2

Numbers and percentage of the total of labeled neurons in the thalamus after injections in motor areas. Results are from two cases with horizontal thalamic sections (see figure 13-1,15-1,17-1, and 18). A. A bar graph of the percent of labeled neurons in each thalamic region. B. The number of neurons and the percent of the total for each thalamic region.

A

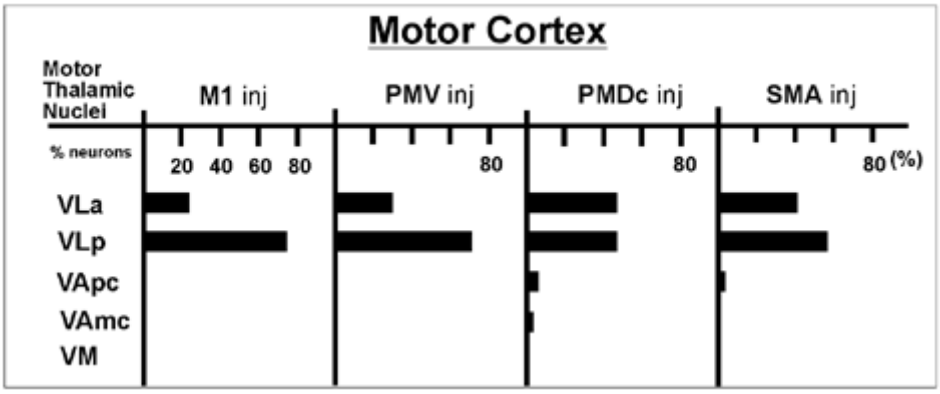

B

Motor Cortex Motor Thalamus	M1 FL (03-74)	PMV OF(03-65)	PMDc FL(03-65)	SMA FL(03-74)
VLa	81 (24)	108 (30)	355(46)	653 (40)
VLp	260 (76)	253 (70)	348(46)	970 (58)
VApc	0 (0)	4 (0)	43(6)	36 (2)
VAmc	0 (0)	0 (0)	14(2)	0 (0)
VM	0 (0)	0 (0)	5(0)	7 (0)
Total	341	365	765	1666

Table 3

Subdivisions of motor thalamus in monkeys and galagos.

Major division	**VA**		**VL**				**VM**
			anterior	**posterior**			
Macaque monkey (Olszewski, 1952)	VAmc	VApc	VLo	VPLo	Area X	VLc	VLm
Jones (1985)	VAmc	VAp	VLa		VLp		VMp
Owl monkey (Stepniewska et al., 1994)	VAmc	VApc	VLa	VLp	VLx	VLd	VM
Galago	VAmc	VApc	VLa	VLp(dorsolateral,posterior,anteromedial)			VM